UPTEC X 06 035
AUG 2006

ISSN 1401-2138

PIA DAMM

Insulin-like growth factor II and its mimetic peptides

Master's degree project

UPPSALA UNIVERSITET

Molecular Biotechnology Programme

Uppsala University School of Engineering

UPTEC X 06 035	Date of issue 2006-08

Author

Pia Damm

Title (English)

Insulin-like growth factor II and its mimetic peptides

Title (Swedish)

Abstract

The insulin-like growth factor I and II (IGF-I and -II) are structurally similar polypeptides with neurotrophic effects, particularly important in the development of the nervous system. The actions of both factors are mainly mediated through the IGF-I receptor (IGF-IR). However, the knowledge of the IGF-II IGF-IR interaction is very limited. In this master's thesis IGF-II was characterized by studying the ability of IGF-II derived peptides to bind to IGF-IR and differentiate neurons. Four peptides were found to exhibit neuritogenic effect and two of those shown to bind to the IGF-IR, but also to the IGF-II receptor (IGF-IIR) and the insulin receptor (IR). Thus, the peptides contain IGF-II sites responsible for binding to and activation of IGF-IR, as well as binding to IGF-IIR and IR. Impairment in IGF-I and IGF-II signaling has previously been observed in several neurodegenerative disorders and in relation to this, the IGF-II mimetic peptides may serve as a therapeutic rescue.

Keywords

IGF-II derived peptides, neuritogenesis, binding sites, IGF-I receptor activation, neurodegenerative disorders

Supervisors

Elisabeth Bock and Vladimir Berezin

Protein Laboratory, Institute of Molecular Pathology, University of Copenhagen

Scientific reviewer

Dan Lindholm

Institute of Neuroscience, Uppsala University

Project name	Sponsors
Language **English**	Security
ISSN 1401-2138	Classification
Supplementary bibliographical information	Pages **65**

Biology Education Centre Biomedical Center Husargatan 3 Uppsala

Box 592 S-75124 Uppsala Tel +46 (0)18 4710000 Fax +46 (0)18 555217

Insulin-like growth factor II and its mimetic peptides

Pia Damm

Sammanfattning

Insulinliknande tillväxtfaktor-I och -II (IGF-I och -II) är homologa proteiner som är viktiga vid utvecklingen av centrala nervsystemet då de framkallar mognad och tillväxt av nervceller. Växtfaktorernas effekt förmedlas framförallt genom IGF-I receptorn (IGF-IR), men även genom insulin receptorn (IR) och IGF-II receptorn (IGF-IIR). IGF-IRs tredimensionella struktur har ännu inte blivit klargjord och därmed har bindningsställena mellan IGF och IGF-IR är inte heller helt definierats, även om bindningen mellan IGF-I och IGF-IR har undersökts till en viss del. Baserat på IGF-IIs roll i hjärnans utveckling, vore det intressant att undersöka hur proteinet förmedlar sin effekt, dvs. undersöka vilka delar av IGF-II som binder till och aktiverar IGF-IR. I det här examensarbetet karaktäriserades IGF-II genom att studera hur peptider, skapade utifrån IGF-IIs struktur, binder till IGF-IR samt stimulerar utveckling av nervceller från lillhjärnan. Fyra av peptiderna framkallade mognad av nervceller och två av dessa uppvisade dessutom bindning till IGF-IR, dvs. de motsvarar potentiellt IGF-IIs bindningsställen till IGF-IR. Emellertid band peptiderna även till IGF-IIR och IR, vilket tyder på att de IGF-II bindningsställen som peptiderna innehåller är gemensamma för alla tre receptorer.

Tidigare studier har visat att IGF-I och –II signalering är nedsatt hos patienter med neurodegenerativa sjukdomar, därför kan IGF-II mimikerande peptider eventuellt ha terapeutisk potential.

Examensarbete 20 p i Molekylär bioteknikprogrammet

Augusti 2006

Abbreviations

AD	Alzheimer's disease
ANOVA	analysis of variance
AT	ataxia-telangectasia
BCA	bicinchonic acid
BSA	bovine serum albumin
CGN	cerebellar granule neuron
CNS	central nervous system
CR	cysteine rich
DMEM	Dulbecco's modified Eagel's medium
EDTA	ethylene diamine tetraacetic acid
ER	endoplasmatic reticulum
Erk	extracellular signal-regulated kinase
Erk MAPKK	Erk mitogen activated protein kinase kinase
F3	fibronectin type 3
FCS	fetal calf serum
GAP-43	growth associated protein-43
GH	growth hormone
Grb2	growth-factor receptor-bound protein 2
GSK-3β	glycogen synthase kinase-3β
HRP	horseradish peroxidase
Ins	insert domain
IGF-I	insulin-like growth factor I
IGF-IR	IGF-I receptor
IGF-II	insulin-like growth factor II
IGF-IIR	IGF-II receptor
IGFBP	insulin-like growth factor binding proteins
IR	insulin receptor
IR-A	IR isoform A
IR-B	IR isoform B
IRS	insulin receptor substrate
MAPKK	mitogen activated protein kinase kinase
NCAM	neural cell adhesion molecule
NSB	non-specific binding
NSILA	non-suppressible insulin-like activity
NMR	nuclear magnetic resonance
PBS	phosphate-buffered saline
PI3	phosphatidylinositol-3
PTB	phosphotyrosine binding
PH	pleckstrin homology
RU	resonance units
RER	rough ER
SCA-I	spinocerebellar ataxia I
SDS	sodium dodecyl sulphate
SDS-PAGE	SDS-polyacrylamide gel electrophoresis
SEM	standard error of the mean
SH2	src-homolog and collagen like protein 2
SPR	surface plasmon resonance
TGFβ	transforming growth factor β
Tg	transgenic
wt	wild type

Contents

Chapter 1

Introduction

The homologous polypeptides insulin-like growth factor type I and type II (IGF-I and II) are widely expressed in the central nervous system (CNS) during development, where their temporal and spatial distribution suggest that they play an important role in brain development. More specifically, the IGFs induce neuronal proliferation, differentiation and survival. Furthermore, the expression of both IGF-I and IGF-II is increased in brain injury and the IGF-I has been shown to prevent neuronal apoptosis *in vivo* and *in vitro*.

These actions of IGF-I and IGF-II are mediated by the IGF-I receptor (IGF-IR). The binding sites of IGF-I to the IGF-IR have been studied to some extent. However, the knowledge of the binding site(s) of IGF-II to the IGF-IR is very limited. Based on the effects of IGF-II activated IGF-IR, it would be of interest to find the important sites of IGF-II for binding and activation of the IGF-IR. In a longer perspective the characterization of the structure-function relationship of IGF-II is of importance as it may have an impact on a number of neurodegenerative diseases caused by impaired IGF-I signaling.

The characterization of IGF-II induced neuronal differentiation was investigated in this master thesis, using five IGF-II derived peptides. Peptides are valuable as research tools when investigating the interactions and biological effects of proteins, which was the purpose of these studies. The results suggest that four peptides have neuritogenic potential and three of those peptides exhibit binding to the IGF-IR. However, when characterizing differentiating effects of IGF-II, it should be taken into consideration that the IGFs and the IGF-IR exhibit significant similarity in sequence and structure with insulin and the insulin receptor(IR), respectively. This results in cross-talking between the systems and overlapping functions of the receptors. For example, IGF-II is a bifunctional ligand as it is able to stimulate both IR and IGF-IR to mediate prenatal growth. Postnatally, the IR

mediates metabolic effects induced by insulin binding. Thus, the potential binding of the IGF-II to the IR and its outcomes should be kept in mind when investigating binding sites in IGF-II. In order to give a better understanding of the insulin/IGF family, the structure and biological functions of its ligand and receptor members will now be outlined together with the presentation of the role of impaired IGF-I signaling in neurodegenerative disorders.

Chapter 2

Theoretical background

2.1 Insulin/IGF family ligands

The IGFs were discovered in 1957 by Salmon and Daughaday, who proposed that growth hormone (GH) itself does not stimulate growth processes *in vivo*, but that GH actions are mediated by secondary agents [Salmon and Daughaday, 1957]. These agents were initially named sulfation factors as they were identified based on their ability to stimulate cartilage sulfation. In the 1970's further characterization of these factors led to recognition of their multiple actions such as stimulation of synthesis of DNA, proteoglycan and protein. These new characteristics led to the renaming of the sulfation factors to somatomedins [Daughaday et al., 1972]. Parallel to the characterization of the sulfation factors, studies were conducted with the aim of identifying factors in serum, which could simulate the effects of insulin. These factors were distinct from insulin since their actions could not be abolished by anti-insulin anti-body, and they were therefore termed non-suppressible insulin-like activity (NSILA) [Froesch et al., 1966]. Based on the structural and functional resemblance to insulin, these molecules were finally defined as insulin growth factor I and II [Rinderknecht and Humbel, 1978b,a].

Together with insulin, IGF-I and IGF-II comprise the ligands of the insulin/IGF family. Insulin, which exhibits 48 % similarity in amino acid sequence to the IGFs, had a great impact on diabetes treatment when it was identified by Banting and Best in 1921. The molecule was first synthesized in the early sixties [Du et al., 1961; Katsoyannis, 1967; Zahn, 2000] and the location of its synthesis, the β-cells of the pancreas, was found a few years later [Steiner, 1969; Steiner et al., 1967]. Finally, the three dimensional structure of insulin has been established using x-ray [Blundell et al., 1971; Baker et al., 1988].

2.1.1 Biological actions

The IGF-I and IGF-II have growth promoting effects as well as insulin-like metabolic activities, most of which are mediated through the IGF-IR [Stewart and Rotwein, 1996]. In terms of effects on neuronal cells, the IGFs were until rather recently mainly recognized for their metabolic effects. First, in the 1990s', IGF-I was described as a neuronal survival factor [Dudek et al., 1997]. It was demonstrated that IGF-I and IGF-II play a significant role in brain development [D'Ercole et al., 1996a]. Altogether, these findings led to the suggestion that IGF-I and II are important determinants of neuronal health and disease.

The neurotrophic effects of IGF-I have been further characterized as promoting proliferation and differentiation of developing neuronal cells [Guan et al., 2003; Khandwala et al., 2000; Pollak et al., 2004]. In addition to its role in proliferation and maturation, *in vitro* and *in vivo* studies have shown that IGF-I promotes survival and prevents apoptosis in neuronal cells [Yin et al., 1994; Delaney et al., 2001]. Besides its effects on neuronal cells, IGF-I is an important factor for the survival, development and myelination of oligodendrocytes [Ye et al., 2002].

The role of IGF-II in postnatal brain development is less understood, but it has been proposed that IGF-II plays a role in differentiation and proliferation in the CNS [Kiess et al., 1994]. In cultured neuroblastoma, sensory, sympathetic and motor neurons IGF-II have demonstrated to support neurite growth [Near et al., 1992]. Similarly to IGF-I, the IGF-II is associated with oligodendrocytes and myelin, which implies its role in myelination [Logan et al., 1994].

The roles of IGF-I and -II have been affirmed by studies of transgenic (Tg) mice that overexpress and knock out mice that do not express IGF-I and IGF-II. Mice overexpressing IGF-I have significantly larger brains, whereas mice overexpressing IGF-II have only thymus overgrowth suggesting an effect of IGF-II on thymic development [Chrysis et al., 2001; van Buul-Offers et al., 1995]. The cerebellar overgrowth in the IGF-I Tg mice is most likely attributable to IGF-I inhibition of granule cell apoptosis [Chrysis et al., 2001]. Conversely, IGF-I knock out mice have a marked reduction in neural cell number, deficiencies in myelination and increased neuronal apoptosis. This is associated with severe retardation and impairment of brain growth and development [de la Monte and Wands, 2005]. Deficiency of IGF-I has also occurred in one case in human. Here, the unique signaling outcomes of the IGF-I and IGF-II ligands were evident as the IGF-II was not able to compensate for the lack of IGF-I, leading to severe growth retention and mental retardation. This occurred despite of the high structural similar-

ity between IGF-I and IGF-II [Woods et al., 1997; Denley et al., 2005b; Walenkamp et al., 2005].

Insulin is involved in regulation of glucose homeostasis. In the CNS, insulin plays an important role in appetite regulation, learning and memory, fertility and reproduction [Stockhorst et al., 2004]. These actions are mediated through the insulin receptor.

2.1.2 Expression

IGF-I is mainly found in maturing neurons in the embryonic and adult brain, especially during postnatal development, Additionally, IGF-I is expressed in activated microglia and macrophages in response to injury. Furthermore, upon the stimulation of GH, IGF-I is synthesized peripherally in the liver. The IGF-I expression declines in the adult rodent, but is consistent in the human brain [Bondy and Cheng, 2004; Nakae et al., 2001].

Similarly to IGF-I, IGF-II is expressed in various regions of the fetal and adult brain, mainly in the non-neuronal cells of mesenchymal and neural crest origin [D'Ercole et al., 1996b]. In addition, the IGF-II expression has been shown to be induced in the developing brain during wound repair following hypoxic ischemic injury, suggesting its role in neuroprotection [Beilharz et al., 1995].

The source of insulin in the brain has been under discussion. Some studies suggest that insulin produced in the pancreatic β-cells is transported across the blood-brain barrier into the cerebrospinal fluid through receptor-mediated uptake [Poduslo et al., 2001]. This peripherally synthesized insulin is regulated by nutrient stimuli. Other results indicate that the insulin is produced locally in the brain [Wozniak et al., 1993]. The most recent findings suggest that insulin in the brain originates from both local and peripheral sources [Gerozissis, 2003].

2.1.3 Structure

The single chain polypeptides, IGF-I and IGF-II respectively, are classified into four domains: A, B, C and D. The IGF-I consists of 70 amino acids and has a molecular weight of 7649 Da. The IGF-II is slightly smaller, comprised of 67 amino acids, resulting in a molecular weight of 7471 Da. As previously mentioned, the IGFs are structurally related to insulin. More specifically, the A and B domain of the IGFs have 50 % sequence similarity to the A and B chains of insulin [Rinderknecht and Humbel, 1978b]. The three-dimensional structure of IGF-I has been solved both by nuclear magnetic resonance (NMR) and X-ray crystallography methods. Regarding

the IGF-II, fewer studies have been conducted and only NMR structures have been reported. The structures of IGF-I and IGF-II reveal the major secondary structural elements: three α-helices (see Figure 2.1b and 2.1c). One helix is situated in the B domain: B11-B21 (B8-B17 of IGF-I) and the other two are located in the A domain: A2-A7 and A13-A19 (A2-A7 and A13-A19 for IGF-I). The three dimensional folding of the growth factor is held together by disulphide bridges, linking the cysteine residues A6 with A11, A20 and A7 with B21 and B9, respectively (B18 and B6 for IGF-I) [Denley et al., 2005a]. The C domain of the IGF-I and II, composed of 12 and 8 amino acids respectively, does not show any similarity to the C peptide of proinsulin. The D domain is 8 residues long in IGF-I and 6 residues in IGF-II [Rinderknecht and Humbel, 1978b,a]. In solution structures by NMR the D and C domain appear highly flexible [Denley et al., 2005a].

Insulin is a 5802 Da dipeptide, comprised of 51 amino acids arranged in A and B chains. The A chain consists of 21 amino acids arranged in a N-terminal helix linked to an anti-parallel C-terminal helix (A1-A8 and A12-A20). The 30 amino acids B chain has a helical segment centrally located (B9-B19). Similarly to the IGFs the chains are linked by disulphide bridges. More precisely, the N- and C-terminal helices of the A chain are joined to the central helix of the B chain (A7-B7 and A20-B19) [Dodson and Steiner, 1998]. Depending on the concentration and the pH, the peptide exists in solution as monomer, dimer or hexamer. At physiological concentration, < 1 nM, and at neutral pH, insulin exists as the active form of the hormone, i.e. as monomer. However, as pH declines and as concentration increases, the monomers form dimers, which further assembles to hexamers in the presence of zink ions [Derewenda et al., 1989]. The three-dimensional structure of insulin monomers have been reported by X-ray crystallography and NMR (see Figure 2.1a) [Denley et al., 2005a].

(a) Insulin (b) IGF-I (c) IGF-II

Figure 2.1: The structures of insulin (a), IGF-I (b) and IGF-II (c). Insulin B chain is colored red. PDB sources 3FG1, 1IGL and 4INS

2.1.4 Genomic organisation

The genes encoding IGF-I and IGF-II have been assigned by Brissenden et al. [1984]. *igf-I* is located on chromosome 12 and *igf-II* on chromosome 11, where it is connected to the insulin gene. *igf-I* is 90 kbp gene comprising 9 exons (Figure 2.2). There are three mRNAs transcribed from the gene, with different 3' untranslated regions (exon 5 or 6, respectively). Exon 1 is a non-coding region forming the 5' untranslated region, which in the precursor corresponds to the signal peptide. Exons 3 and 4 encode the mature IGF-I (domains BCAD). When transcribed the mRNA results in a precursor of 1.1 kb, 1.3 kb and 7.6 kb depending on the exon combination [Humbel, 1990]. The hepatic expression of *igf-I* is up-regulated primarily by GH, but the stimulatory influence of GH is markedly reduced by malnutrition. The extrahepatic production of IGF-I is influenced by the nutritional state as well as by the developmental stage and the tissue it is expressed in [Khandwala et al., 2000]. The *igf-II* gene is assigned to 11p11. It encompasses 30

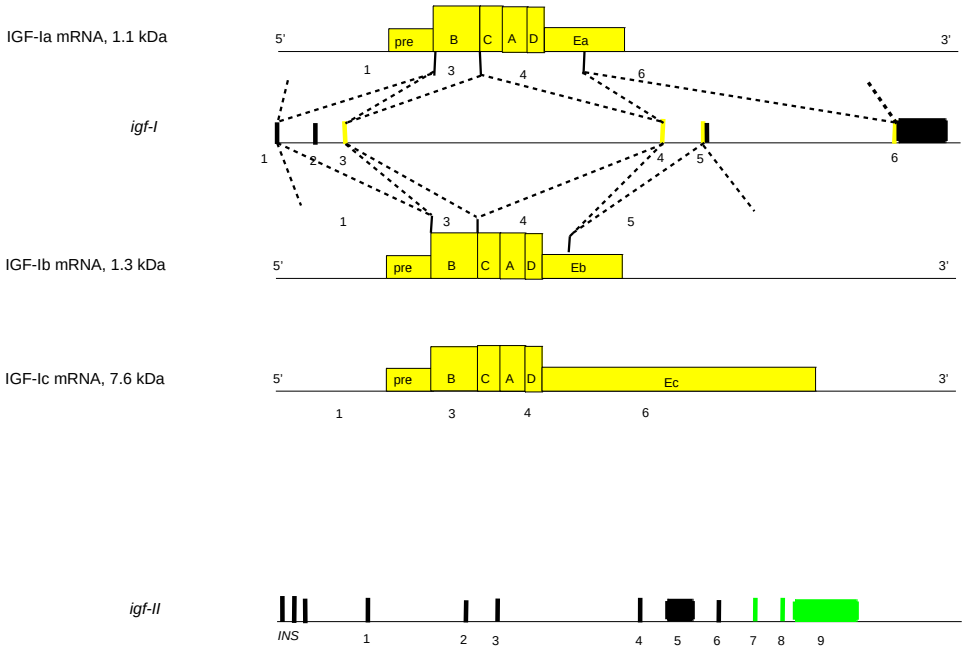

Figure 2.2: Map of the genes encoding IGF-I and IGF-II. Translated regions are colored, untranslated are indicated in black.

kbp and contains nine exons (Figure 2.2). The transcriptional activity is regulated by four promoters positioned in front of exon 1, 4, 5 and 6, respectively. The promoters give in a tissue- and developmental-specific way rise to the pre-pro IGF-II mRNA (encoded in exons 7, 8 and 9). Exon 1-6 are non-coding and yield the leading 5'-untranslated region of the RNA molecules expressed. The pre-pro IGF-II is 113 amino acids longer than the

spliced version of the factor as it contains a carboxy-terminal peptide and signal peptide (89 and 24 amino acids respectively), which are cleaved off post-translationally [Meinsma et al., 1992].

As previously mentioned, the gene encoding insulin, *ins*, is coupled to the *igf-II* gene and located on chromosome 11 (11p15) [Harper et al., 1981] and the gene encompasses approximately 5 kbp. The *ins* gene contains its five exons and two introns [Bell et al., 1980]. The transcribed and translated sequence results in pre-proinsulin, which consists of a signal peptide, the B chain, the C peptide connecting the B and A chain, and the A chain. The signal peptide is removed when the pre-proinsulin crosses the membrane of the endoplasmatic reticulum (ER). Proinsulin is formed and it is folded to its three dimensional structure. Subsequently, the proinsulin is transported in secretory vesicles from the rough ER (RER) to the Golgi apparatus. Here enzymes, acting outside the Golgi, process the proinsulin into insulin and C-peptide. The mature vesicles, i.e. secretory granules, are secreted into the circulation by exocytosis [Wilcox, 2005]. The C-peptide has recently been shown to promote insulin disaggregation and thereby enhance glucose metabolism [Shafqat et al., 2006]. Furthermore, in the presence of insulin the peptide has the an effect on cell proliferation, neurite outgrowth and survival in high-glucose induced apoptosis in neuroblastoma SH-SY5Y cells [Lie et al., 2003].

2.1.5 Insulin-like growth factor binding proteins

The availability of IGF-I and IGF-II to bind to the insulin/IGF family receptors is modulated both positively and negatively by a family of six high affinity insulin-like growth factor binding proteins (IGFBP). Approximately 99 % of the circulating IGF is normally bound to IGFBPs. The functions of these serum proteins are to increase the half-life of the IGFs and to deliver the IGFs to tissues. In the tissue, IGFBP can either increase the efficiency of the IGFs by releasing IGFs to bind to the receptors, or inhibit the IGF actions by sequestering the IGF from the receptor. Normal growth is a result of the balance of IGF and IGFBR, which fine tunes the accessibility of IGF to bind the IGF-IR [Denley et al., 2005a].

2.2 Insulin/IGF family receptors

In line with the high structural similarity of the ligands IGF-I, IGF-II and insulin, there is significant similarity between the IGF-IR and the IR, which results in overlapping functions of the receptors [Nakae et al., 2001]. As illustrated in Figure 2.3 all three ligands bind to the IGF-I receptor and activate the intracellular tyrosine kinase activity. This yields a variety of responses such as proliferation, differentiation, inhibition of apoptosis and migration.

The IGF-IR is encoded by the 21-exon *igf1r* gene, on chromosome 15 in human (15q25). The extracellular 607 amino acid α-subunit and the 626 amino acid transmembrane β-subunit have molecular weight of 135 and 95 kDa, respectively. The IR exists in two isoforms, IR-A and IR-B, differing in the

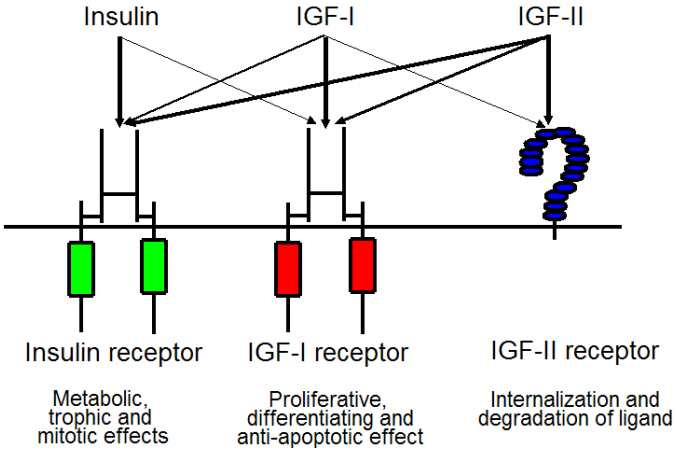

Figure 2.3: IGF/Insulin family receptors and their ligands. The thickness of the arrows indicate the affinity of the ligand to bind to the respective receptor (thicker arrow corresponds to higher affinity).

number of amino acids of the α-subunit due to alternative splicing of exon 11 of the *INSR* gene. The IR-B isoform, which includes exon 11, has low affinty for the IGFs and high affinity for insulin, which induces metabolic responses upon binding to the receptor. Conversely, it has recently been demonstrated that the resulting IR-A isoform has high affinity for insulin as well as for IGF-II, and that activation of the IR-A leads to mitogenic responses similar to those of IGF-IR [Denley et al., 2003]. The *INSR* gene comprise 22 exons (11 for each α- and β-subunit) separated by 21 introns. Human *INSR* is located on chromosome 19 (19p13) and stretches over 130 kbp [Ebina et al., 1985]. The α-subunit of insulin is formed by translation of mRNA to either 719 or 731 amino acids depending on the tissue specific alternative splicing of the 36 bp exon 11. The β-subunit consists of 620 amino acids [De Meyts, 1994].

The IGF-IR and IR are expressed throughout the CNS. There is a great overlap in the expression of the two receptors such as in the olfactory bulbs, cerebellar cortex and hippocampal formation. However, there are also specific cell populations with selective enrichment for IR or IGF-IR expression. The anterior thalamic and hypothalimic nuclei are enriched for IR, whereas the suprachiasmatic nucleus of the hypothalamus and the dorsal thalamic sensory nuclei selectively express the IGF-IR [Bondy and Cheng, 2004]. The receptors are expressed in both fetal and adult brains, and their expression

pattern does not vary during development [de la Monte and Wands, 2005].

The IGF-II receptor (IGF-IIR), also known as the cation-independent mannose-6-phosphate receptor, binds IGF-II and proteins containing mannose-6-phosphate such as proliferin, transforming growth factor β (TGFβ) and renin. The IGF-IIR does not have an intrinsic signaling domain. Instead, its major function is to clear circulating IGF-II and thereby modulate the availability of the ligand to the IGF-IR and IR. This is achieved by sequestering the ligands, internalization of the ligand receptor complex and final degradation of the ligands. Since the receptor also binds and proteolytically activates the growth inhibitor TGFβ, it has an additional IGF-independent role in regulating cell proliferation. 90-95 % of the IGF-IIRs are membrane bound in the trans-Golgi network, where their function is to translocate newly synthesized lysosomal enzymes to lysosomes [Scott and Firth, 2004; Denley et al., 2003; Jones and Clemmons, 1995].

The gene encoding IGF-IIR, *M6P/igf2r*, is in humans localized on the long arm of chromosome 6 (6q25)[Humbel, 1990]. The translation of the gene results in a 188 amino acid protein, of which 23 amino acids make up the transmembrane domain and the remaining 163 amino acids the intracellular domain. Altogether, the receptor has a molecular weight of 300 kDa [Stewart and Rotwein, 1996]. The IGF-IIR is expressed in the frontal cortex, hippocampus and cerebellum of fetal and adult human brains [Kar et al., 2006].

2.2.1 Structure and binding sites

The IGF-IR and IR are disulphide-linked dimers, where each half consists of a ligand binding α-subunit disulphide-linked to a transmembrane β-subunit. Similarly to the IR, the α and β-subunits of the IGF-IR are produced from a pre-proprotein, which is glycosylated and proteolytically processed to result in separate α and β chains. The extracellular α-subunits form through disulphide bridges a β-α-α-β arrangement with the two membrane spanning β-subunits (see Figure 2.4). As ligand binds to the α-subunits, conformational changes occur leading to tyrosine phosphorylation of the intracellular part in the β-subunits. The phosphorylation yields an increase in the intrinsic kinase activity of the receptor [Denley et al., 2005a]. The major feature that distinguishes the IGF-IR and the IR from most other receptor families is that they occur on the cell surface as disulphide-linked dimers and require domain rearrangements, as opposed to receptor oligomerisation, to initiate signal transduction.

The complete structure of neither the IR nor the IGF-IR have been established to date. However, the structures of the three outermost extracellular

domains of the IGF-IR have been determined. The L1 domain and the cysteine rich (CR) domains of the IGF-IR have been shown to be important for IGF-I binding, whereas only the L1 domain is critical for IGF-II binding to the IGF-IR (domains illustrated in Figure 2.4). In addition, certain residues (692-702) in the insert domain (Ins), positioned at the C-terminus of the α-subunit, are necessary for binding of the two ligands. The binding sites of the IR-A and the IR-B are similar to those of the IGF-IR, including L1 and Ins, but also the L2 domain [Denley et al., 2005a].

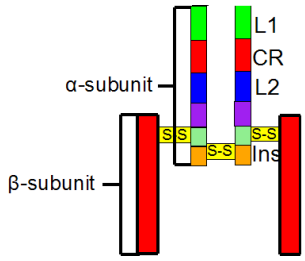

Figure 2.4: Binding domains in the IGF-IR and IR. CR, cysteine rich domain; Ins, insert domain.

The reported binding affinities of the ligands to the receptors vary a great deal depending on the experimental set up. For example, the reported binding affinity of IGF-I to its cognate receptor IGF-IR vary up to 100-fold depending on the assay used. However, the relative binding affinities of the receptors for the different ligands are consistent between the studies. Jones and Clemmons [1995] reported that IGF-IR binds IGF-I with approximate K_D value of 1 nM. The affinity of the receptor for IGF-II is two-three fold lower and approximately 100- to 1000 fold lower for insulin. The IR isoforms bind insulin with an affinity of 0.2-1 nM and demonstrated a 100-fold lower affinity for IGF-I. The IR-A binds IGF-II with only 5-fold lower affinity than it binds insulin. The other IR isoform, IR-B, has approximately 30-fold lower affinity for IGF-II than for insulin [Forbes et al., 2002; Denley et al., 2005a].

IGF-IIR is a monomeric receptor with a large extracellular domain consisting of 15 repeat sequences, a transmembrane domain and a intracellular domain. The binding sites of IGF-II are distinct from that of mannose-6-phosphate, as the IGF-II binds first and foremost to domain 11 and secondly to domain 13, whereas the mannose-6-phosphate proteins bind to domains 1-3 and 7-9 [Stewart and Rotwein, 1996]. The affinity constant of IGF-IIR for IGF-II is, according to Denley et al. [2005a], 0.2 nM. The receptor interacts minimally with IGF-I, which is revealed by the high K_D value, 0.4 μM. Insulin does not bind to the IGF-IIR [Denley et al., 2005a].

2.2.2 IGF and insulin signaling

IGF and insulin induced signaling is initiated when the IGF-I, IGF-II or insulin binds to either IGF-IR or IR, leading to activation of the intracellular receptor tyrosine kinases. These kinases phosphorylate several cytosolic molecules such as the insulin receptor substrate (IRS) molecules. The IRS are organized in four subtypes, but common to all IRS is that they consist of a highly conserved N-terminus and a more variable C-terminus that carries multiple phosphorylation sites. The N-terminal region contains three functionally important domains. Firstly, one domain with homology to pleckstrin (PH) mediates IRS interactions with Janus tyrosine kinase Tyk-2 and possibly signals through G proteins and phospholipids. Secondly, two domains with phosphotyrosine binding (PTB) domain homology that interact with the IR and IGF-IR. The less conserved C-terminus interacts with proteins containing src homology 2 (SH2) domains. Thus, the signal specificity is determined by the IRS molecules PTB domain binding to the receptor and the selective interactions between IRS molecules and SH2 domain-containing proteins, which mediate specific cellular responses [Giovannone et al., 2000].

The interaction between the IRS and SH2 domain containing molecules occurs first after the residues on the IRS C-terminus have been phosphorylated by receptor tyrosine kinases. Growth-factor receptor-bound protein 2 (Grb2) is one of the SH2 domain molecules, which upon binding to IRS activate the Erk mitogen activated protein kinase kinase (Erk MAPKK) pathway. The Erk MAPKK activation results in insulin- and IGF-I stimulated mitogenesis, neurite sprouting, and gene expression. Alternatively, the IRS may bind to the p85 regulatory subunit of phosphatidylinositol-3 kinase (PI3 kinase), which leads to glucose transport and inhibition of apoptosis through the Akt/Protein kinase B pathway. More specifically, the Akt kinase phosphorylates the glycogen synthase kinase-3β (GSK-3β) and BAD, thereby inactivating them. BAD acts pro-apoptoticly by inactivating anti-apoptotic Bcl-family proteins.

Although the signaling pathways downstream of IR and IGF-IR are principally very similar, their functions are not entirely equal and the receptors are expressed differently in cell populations in the developing, mature and aging CNS as described on page 12. The biological effect of activation of a receptor varies in different cell types, to a large extent due to the availability of substrates. For example, the IGF-IR mediates differentiation signals upon IGF binding in the absence of IRS-I. Conversely, in the presence of IRS-I the signal is mitogenic [Valentinis and Baserga, 2001]. The insulin expression is highly regulated by nutrient stimuli and therefore fluctuates, as opposed to the IGF expression which is rather constant. This results in continuous activation of IGF-IR and transient activation of IR, which may effect the

downstream signaling [Blakesley et al., 1996; De Meyts et al., 1995]. The specificity in signaling has also been explained by the difference in binding kinetics and the period of time the ligand is bound to the receptor, which effects the down stream signaling. E.g. insulin analogues with slow dissociation rate from the IR induce mitogenic effect, whereas the wild type (wt) insulin activation of the IR results in metabolic actions [De Meyts, 1994].

2.3 Neurodegenerative disorders and impaired IGF-I signaling

Many neurodegenerative disorders are related to a change of IGF-I levels in serum and brain, and as IGF-I has a neuroprotective role when signaling through the IGF-IR, it has been hypothesized that degeneration of neurons is due to impaired IGF-IR signaling [Trejo et al., 2004]. Based on the fact that IGF-II binds and activates the IGF-IR and potentially plays a role in protection against apoptosis, as suggested in section 2.1.2, peptides derived from the IGF-II may mimic the IGF-II signaling through IGF-IR and potentially have a therapeutic impact on patients with impaired IGF-IR signaling. The impaired IGF-IR signaling in neurodegenerative diseases will now be outlined.

Several neurodegenerative disorders exhibit reduced IGF-IR signaling, which is most likely due to desensitization of nerve cells to IGF-I. It is important to determine whether the desensitization to IGF-I is the cause of the degenerative disease or if it has developed as a consequence of the neuronal damage. The former alternative appears to be the case in disorders such as ataxia-telangectasia (AT) and spinocerebellar ataxia I (SCA-I). In AT, a mutation in the *ATM* gene leads to low expression of the IGF-IR resulting in loss of sensitivity to IGF-I. and in SCA-I patients the PI3/Akt signaling modulates the neurotoxicity of ataxin. [Chen et al., 2003; Humbert et al., 2002] A therapeutic rescue to patients with these disorders could potentially be IGF-I or IGF-II sensitizers. The other scenario, where dysfunctional IGF-IR signaling is a secondary process adding to the pathological cascade, is probably the most likely situation in most neurodegenerative diseases. In this case, the primary defect could be inflammation, environmental toxins, ethanol consumption or hepatic dysregulation due to diabetes [van Dam and Aleman, 2004].

The signaling stimulated by IGF-I, IGF-II and insulin is also impaired in Alzheimer's disease (AD) and it has been suggested that this abnormality is the underlying basis of the disease. More specifically, the neurodegeneration is mediated by depletion of IGF/insulin leading to increased levels of GSK-3β, yielding neuronal oxidative stress and cell death [de la Monte and

Wands, 2005]. The authors suggest IGF-I, IGF-II and insulin sensitizers (CNS specific) to be the most preeminent form of therapeutic rescue in the early and intermediate stage of the disease. Conclusively, for patients with neurodegenerative disorders caused by malfunction in IGF-I signaling, the therapeutic rescue could be provided by IGF-I, IGF-II and insulin sensitizers, to enhance the neuronal survival and reduce the oxidative stress. The IGF-II derived peptides could potentially act as IGF-I/IGF-II sensitizers.

2.4 IGF-II derived peptides

In order to get a better understanding of the functions of a protein, studies can be conducted using peptides designed to mimic the actions of the protein. These mimetic peptides can be designed using one of two methods: by the use of combinatorial peptide libraries or by *in silico* modeling. The first alternative involves peptides synthesized by combinatorial chemistry. These are then examined for their ability to function as the cognate protein. It should be noted that these methods may yield a peptide, which induces similar biological effects as the cognate protein, but without sharing the same protein sequence. The latter alternative is based on studies of the three dimensional structure of the protein obtained by NMR or X-ray crystallography. These structures allow predictions of functional domains in the protein, upon which peptides can be synthesized.

Primarily, the peptides function as research tools. For example, they can be used to study the biological functions of a protein and they are very useful for deciphering which parts of the proteins are responsible for different functions. An example of this is a number of peptides derived from the neural cell adhesion molecule (NCAM), which have been reported to exhibit unique biological profiles and mimic specific functions of NCAM [Berezin and Bock, 2004].

For the present study, five IGF-II derived peptides have been synthesized to aid the characterization of the binding of IGF-II to the IGF-IR. The design of the IGF-II derived peptides is based upon potential binding sites for IGF-II to IGF-IR, some of them being homologous to the potential binding sites for IGF-I to IGF-IR. As described in section 2.1.1, IGF-II induces differentiation and proliferation in developing neurons. The homologous IGF-I has, apart from these actions, an effect on neuronal survival and it is hypothesized that IGF-II derived peptides could exhibit similar effects on neurons. Moreover, the IGF-II is also structurally related to insulin and it has been shown that IGF-II binds to the IR-A, which upon IGF-II binding, mediate survival, proliferation and migration, displaying similar effects to the effects mediated by the IGF-IR. This suggests yet another potential role of the

peptides: they may bind the IR and induce mitogenic effects on neurons. However, the primary purpose of the design of the peptides was to study the differentiating effect of IGF-II via IGF-IR.

Studies using the IGF-II derived peptides could reveal binding sites as well as the functional relevance of the binding sites. Furthermore, if any of the peptides activate the receptor upon binding, they may be of interest when developing low molecular weight agonists. In a longer perspective, the peptides may be a potential drug candidate for patients suffering from neurodegenerative disorders, for example acting as IGF-I sensitizers as suggested in section 2.3.

2.5 Surface plasmon resonance

In the characterization of IGF-II, binding studies were conducted employing a Biacore 2000 and a BIAlite instrument as described further in section 4.2.4. The instruments utilize the phenomenon surface plasmon resonance (SPR) to study the interaction between molecules in real time. SPR occurs in thin metal films positioned between media of different refractive index. In Biacore and BIAlite systems the media are glass and sample solution, respectively, and the film is a thin layer of gold.

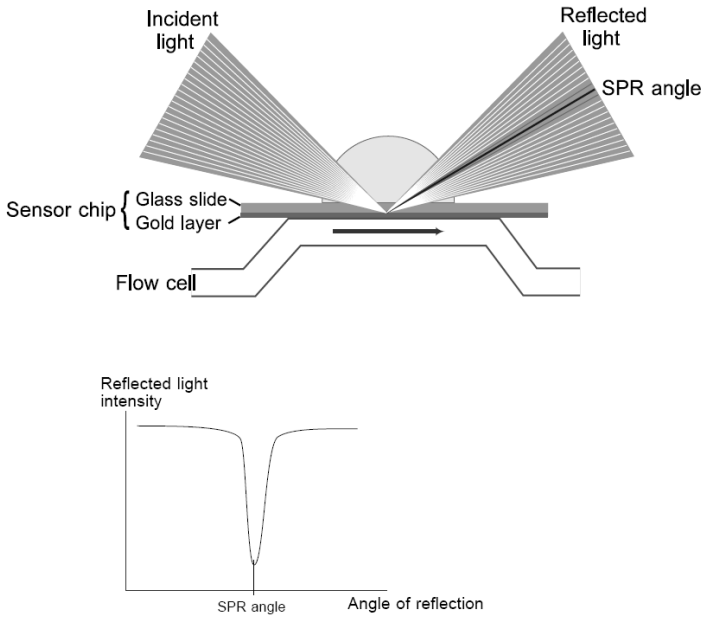

Figure 2.5: The principle of SPR. Illustration used with permission from Biacore AB [Biacore Sensor Surface Handbook, version AA, 2003]

As light, coming through media with higher refractive index, strikes the interface at an angle beyond the critical angle, all light is reflected back (100 % reflection) and an electric field intesity, called an evanescent wave field, is generated from the light.At a specific angle and wave length the evanescent wave interacts with, and is absorbed by the free electron clouds in the gold layer resulting in electron charged density waves known as plasmons. This leads to a reduction in the intensity of the reflected light, which characterizes the SPR angle. The evanescent field wave travels a short distance in the solution and the conditions for SPR are very sensitive to changes in the solution, e.g. changes in the refractive index. The refractive index of the solution can be changed by alterations in solute concentration at the surface of the sensor chip, which causes the SPR angle to change. By these means the mass change in the solution can be detected in real time. The interaction studies are performed by immobilizing one of the interacting molecules covalently on a dextran covered sensor chip and passing the other interacting molecule over the surface. The interaction is monitored through SPR, as illustrated in Figure 2.5. Binding of molecules to the immobilized molecule will yield a response, measured in resonance units (RU). This response is illustrated in a sensorgram, where RU is plotted against time. In the sensorgram, the interaction can be divided in two phases (see Figure 2.6): the association phase, which starts after injection of the analyte, and the dissociation phase, beginning when the injection is finished [Biacore Sensor Surface Handbook, version AA, 2003].

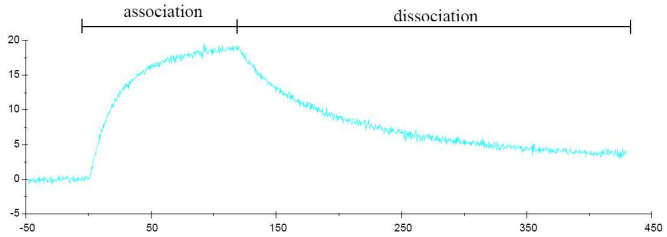

Figure 2.6: Sensorgram. Association phase and dissociation phase are indicated. Illustration used with permission from Biacore AB [Biacore Sensor Surface Handbook, version AA, 2003]

Chapter 3

Aims

The aim of this study was primarily to examine the neuritogenic potential of the IGF-II derived peptides. Furthermore, by employing SPR analysis, it was the aim to study the interactions of the peptides to the IGF-IR, IGF-IIR and IR in order to find potential binding sites. More specifically, it was investigated if the peptides bound to any of the receptors and if so, whether the binding corresponded to a binding site common to all receptors or specific to one receptor.

As the project proceeded, it was indicated that some of the peptides induced neuronal differentiation. Therefore, it also became an aim to investigate the ability of the peptides to phopsphorylate the IGF-IR, and preliminary results from these studies are also presented.

Chapter 4

Materials and methods

4.1 Materials

4.1.1 Chemicals and media

HEPES, B27 supplement, glutamax, penicillin, streptomycin, ampicillin, Trypsin-ethylene diamine tetraacetic acid (EDTA) and Neurobasal medium was purchased from Gibco BRL (Paisley, UK). β-mercaptoethanol was from Hercules (CA, USA). Trypsin, DNAase I, Soybean trypsin inhibitor, bovine serum albumin (BSA), saponin, magnesium sulphate, sodium dodecyl sulphate (SDS), EDTA and Tris were from Sigma-Aldrich (St Louis, MO, USA). Sodium azide was from Bie and Berntsen (Rødovre, Denmark) and Bicinchonic acid (BCA) protein assay reagents and albumin standard were purchased from Pierce (Rockford, USA). Glycine, sucrose, Tween-20, hydrochloric acid, calcium chloride, sodium chloride, glycerol and formaldehyde were from Merck (Darmstadt, Germany). Ethanol was from De Danske Spritfabriker (Copenhagen, Denmark). Phosphate-buffered saline (PBS), Dulbecco's modified Eagel's medium (DMEM), LB broth and Krebs buffer were from the Panum substrate department (Copenhagen, Denmark). Fluorescent mounting medium was from Dako (Glostrup, Denmark). Phosphatase Inhibitor Cocktail Set II was from Calbiochem (La Jolla, USA) and the Complete Protease Inhibitor Cocktail from Boehringer (Mannheim, Germany). Amine coupling kit, HBS-EP (research grade) and BIAmaintenance kit were purchased from Biacore AB (Uppsala, Sweden). Endofree Plasmid Maxi Kit was purchased from Qiagen (West Sussex, UK). EZ-ECL Chemiluminescence Detection Kit for HRP was from Biological Industries Ltd. (Kibbutz Beit Haemek, Israel). NP-40 and ampicillin were from Calbiochem (Darmstadt, Germany) and tetrasodium pyrophosphate was from Fluka (Buchs, Swizerland). Skim milk was purchased from Becton, Dickinson and Company (Maryland, USA). Targefect F-2 was obtained from Targing Systems (CA, USA).

4.1.2 Antibodies, growth factors and receptors

Fetal calf serum (FCS) was purchased from Gibco BRL (Paisley, UK). Recombinant human insulin from Sigma-Aldrich (St Louis, MO, USA). The horse radish peroxidase (HRP) conjugated swine anti-rabbit and goat anti-mouse antibodies were from Dako (Glostrup, Denmark). Polyclonal rabbit anti-rat GAP-43 was purchased from Chemicon Int. Inc. (CA, USA) and Alexa Fluor goat anti-rabbit IgG antibodies conjugated to Alexa 568 was from Molecular Probes (Lieden, Netherlands). Polyclonal rabbit anti-IGF-IRβ (C-20), rabbit anti-IGF-IRβ (C-60) and Protein A/G PLUS Agarose were from Santa Cruz Biotechnology Inc (CA, USA). Monoclonal anti-phosphotyrosine antibody PY20 was from BD Transduction Laboratories (CA, USA). The recombinant human carrier free IGF-I, IGF-II, IGF-IR, IGF-IIR, IR were from R and D systems (Oxon, UK). The IGF-I used in IGF-IR activation experiments was from Lifetech (Edgewater, USA).

4.1.3 Peptides

The IGF-II mimetic peptides and the P2d peptide (GRILARGEINFK), purchased from Schafer-N (Copenhagen, Denmark), were synthesized as tetrameric dendrimers composed of four monomers coupled to a lysine backbone. The IGF-II derived peptides were dissolved in sterile distilled water and purified by gel-filtration utilizing Sephadex^{TM} G-10 (Amersham Bioscience, Uppsala, Sweden). The peptide concentration was determined by spectrophotometric measurements of the absorbance at 205 nm. Since the peptides are not patented to this date, their sequences cannot be revealed.

4.1.4 Cell material and plasmids

Human Embryonic Kidney (HEK) 293 cells, obtained from Clontech (CA, USA), were used for transfection with either the expression vector pCMV6-XL4 containing the cDNA encoding the human IGF-IR (Origene, MD, USA), an enhanced variant of the Aequorea Victoria green flourescent protein (pEGFP-N_1) from Clontech (CA, USA) and/or the empty expression vector pcDNA3.1+ (Invitrogen, CA, USA). For transformation, One Shot TOP10 competent cells were used (Invitrogen, CA, USA).

4.2 Methods

4.2.1 Primary cultures of cerebellar granule neurons

CGNs from 7-8 days old Wistar rats (Charlez River, Sulzfeld, Germany) were prepared essentially as described by Schousboe et al. [1989]. In brief, after rat decapitating, the cerebellum was removed and placed in a solution of Krebs buffer with 0.3 % (w/v) BSA, 0.03 % (v/v) $MgSO_4$ and 20mM

HEPES (solution 1). Using a stereomicroscope the cerebellum was cleared from meniges and blood vessels and homogenised by chopping with a scalpel blade. Next, the neurons were dissociated by mild trypsinization (12 min at 37 °C) in solution 1 supplemented with 0.2 mg/ml trypsin. In order to inactivate the trypsin and degrade free DNA, cells were washed with a mix of solutions 1 and 3 (10.5:2), where solution 3 consists of solution 1 supplemented with 0.08 mg/ml DNAase 1, 0.52 mg/ml soybeen trypsin inhibitor and 1.5 mM $MgSO_4$. Following centrifugation (1500 rpm for 2 minutes), the supernatant was discarded and the cells were resuspended in solution 3. Again, the cell solution was centrifuged (100 rpm for 15 seconds) to let tissue pellet, and supernatant was transferred to washing solution (132 μM $CaCl_2$ and 120 μ M $MgSO_4$ in solution 1).

The cells were pelleted by centrifugation and resuspended in Neurobasal medium supplemented with 0.4% (w/v) BSA, 2% (v/v) B27, 0.5 % (v/v) glutamax, 100 U/ml penicillin and 100 μg/ml streptomycin. Subsequently, the cell concentration was determined using a Burker-Turk counting chamber and the cells were seeded in eight-well LabTek Permanox Chamber slides (Nunc, Roskilde, Denmark) to a density of 10 000 cells per well. Peptides or growth factors were added to a final volume of 300 μl/well, and the cells were grown at 37°C, 5 % CO_2 for 24 hours. Medium was added to the untreated controls and P2d peptide was added to the positive controls. P2d has previously been shown to efficiently induce neurite outgrowth at the concentration of 2 μg/ml [Pedersen et al., 2004].

Except for IGF-II-VI, experiments with two different series of concentrations were performed: first series being 0.3, 1, 3, 9, 27 and 81 μg/ml and second series being 0.1, 3, 27 and 243 μg/ml for IGF-II-I, 0.1, 1, 9 and 243 μg/ml for IGF-II-II and 27, 81, 243 μg/ml for IGF-II-III and IGF-II-V. The number of independent experiments carried out using the first concentration series were eight, seven, four, three and six for IGF-II-I - IGF-II-V, respectively. The number of independent experiments conducetd using the second concentration series were five for IGF-II-I and IGF-II-II, four for IGF-II-III and six for IGF-II-V.

4.2.2 Immunostaining

The neurons were immunostained for growth associated protein-43 (GAP-43), which is a membrane protein expressed in all neurons, but at an altered level in neurons involved in axon growth [Skene, 1989]. Neurons were fixed in 4 % formaldehyde (PBS, 8% (v/v) formaldehyde, 0.1 M sodium phosphate, 0.05 M sucrose, 0.4 mM $CaCl_2$), followed by wash with PBS and, subsequently, with PBS supplemented with 1 % BSA. Next, cells were incubated with polyclonal rabbit anti-rat GAP-43 diluted 1:1000 in PBS solution con-

taining 7 % FCS, 50 mM glycin, 0.2 % saponin and 0.02% (v/v) NaN_3. Next day, following wash with PBS and PBS with 1 % BSA, the cells were incubated for 1 hour at room temperature with secondary Alexa Flour 568 goat anti-rabbit antibodies (diluted 1:1000 in PBS with 1 % BSA). Finally, the cells were washed in PBS and mounted with flourescent mounting medium.

4.2.3 Quantification of neurite outgrowth

Images of the neurons were recorded by computer-assisted fluorescent microscopy using a Nikon diaphot inverted microscope (Nikon, Tokyo, Japan) equipped with an epiflourescent attachment and a Nikon Plan 20x objective. The images were taken using a CCD video camera (Grunding Electronics, Germany) and the software program "Prima" (Protein Laboratory, University of Copenhagen, Denmark). Images of approximately 200±20 cells were recorded randomly in order to get a representative collection of the cells in each well [Ronn et al., 2000]. Using the software package "Process length" the length of neuronal processes per cell was quantified. This analysis is based on a stereological approach described by Ronn et al. [2000], where the intersections between the neurites and the test lines of a counting frame are counted and the neurite outgrowth expressed as the number of intersections per cell (see Figure 4.1). This can be interpreted as the absolute length of neurites(L) per cell according to following formula:

$L=\pi dI/2$

where I = number of intersections per cell and d = the vertical distance between two parallel lines in the frame. In these experiments d = 25 μm.

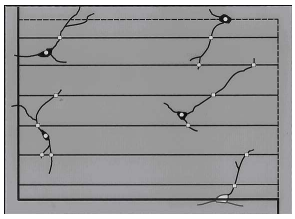

Figure 4.1: The counting frame used for determination of neurite outgrowth. The frame lays over an image of a cell culture. Cells within the frame or touching the hatched lines are counted (black cells), and cells outside the frame or touching the solid lines are excluded (white cells). The intersections between the neurites and the test lines are also marked, resulting in a ratio between the number of intersections and number of cells. Illustration with permission from Ronn et al. [2000]

4.2.4 Surface plasmon resonance analysis

Preliminary binding studies were performed employing a BIAlite instrument (Biacore AB, Uppsala, Sweden) followed by more detailed studies using a Biacore 2000 instrument (Biacore AB, Uppsala, Sweden). The experimental conditions for the two instruments were similar in that the studies were carried out at 25 °C, using HBS-EP buffer containing 0.01 M HEPES pH 7.4, 0.15 M NaCl, 3 mM EDTA, 0.005% (v/v) Surfactant P20 as running buffer and at flow rates 5, 20 or 40 μl/min. For the BIAlite studies a sensor chip CM5 (Biacore AB, Uppsala, Sweden) was used and one type of receptor was immobilized per chip utilizing an amine coupling kit. More specifically, the chip was activated by 30 μl activation solution followed by protein immobilization using 30 μl and 15 μl 10 μg/ml IGF-2 receptor or insulin receptor, respectively, in 10 mM sodium phosphate buffer pH 6 at 5 μl/min. The IGF-I receptor was immobilized using 11 μl 10 μg/ml of the protein in 10 mM acetic acid buffer pH 4 at 5 μl/min. The final receptor density was 4200 RU, 3200 and 3033 RU for IGF-IR, IGF-IIR and IR, respectively.

For the Biacore studies, a sensor chip CM4 (Biacore AB, Uppsala, Sweden) had all three receptor types immobilized essentially as described for the BIAlite experiments. The chip was activated by 35 μl activation solution and protein was immobilized accordingly: 20 μl and 10 μl 25 μg/ml IGF-1 receptor and insulin receptor respectively and 20 μl 50 μg/ml IGF-2 receptor. All receptors were diluted in 10 mM acetic acid buffer pH 4 and injected at 5 μl/min. The final receptor density for the sensor chip CM4 was in the range 1700-4000 resonance units. Finally, both sensor chips CM4 and CM5 were blocked by 35 μl blocking solution. Peptides and growth factors were injected over the sensor chip at indicated concentrations. To test specificity of binding, the peptides were injected at 200 μg/ml over a sensor chip CM5 immobilized with the first and second fibronectin type 3 (F3) module of NCAM and run at 20 μl/min in HBS-EP buffer on the Biacore instrument.

Analysis of the data was performed by non-linear curve-fitting using the software BIAevaluation v.4 (Biacore, Uppsala, Sweden) and/or Origin v.6.1 software (Originlab, MA, USA). All samples were also run over an unmodified flow cell in the sensor chip, thereby enabling low unspecific binding and changes in bulk refractive index to be subtracted. Affinity constants were calculated based upon the curve corresponding to the difference between binding to receptor and the reference flow cell. The curves were fitted to a 1:1 Langmuir binding model, which describes the interaction of two molecules in a 1:1 complex. This model was chosen as the most appropriate, even though the peptides are synthesized as tetrameric dendrimers. The outcome of this will be discussed in section 6.2. The apparent K_D was determined from the calculation ka/kd, where ka is the association rate and kd is the

dissociation rate. Using the Origin v.6.1, analysis was based on the plot of the plateau value of each sensorgram versus the injected concentration of growth factor. The K_D was determined by globally fitting the plot with the interaction model:

$$R_{eq} = R_{max} \times \frac{C}{C+K_D},$$

where R_{max} is the response corresponding to analyte saturation of the surface, R_{eq} is the response at equilibrium and C is the concentration.

4.2.5 IGF-1 receptor phosphorylation

The pCMV6-XL4 vector containing IGF-II cDNA was transfected into One Shot TOP10 competent cells according to the manufacturers directives, plated on agar plates (50 μg/ml Amp) and incubated O/N at 37°C. A single colony was inoculated in LB-broth supplemented with 50 ug/ml ampicillin and incubated at a shaker at 37°C O/N. The plasmid was purified using Endofree Plasmid Maxi Kit as described by the manufacturer.

HEK293 cells were co-transfected using Targefect F-2, according to the manufacturer's instructions, with pcDNA3.1+ or pCMV6-XL4 containing IGF-II cDNA and pEGFP-N_1 (ratio 1:10). Cells were grown in full serum medium for 20-24 hours after transfection, followed by stimulation or starvation for 6 hours in minimal serum medium (0.5% FCS) and stimulation. During stimulation cells were grown in the presence of 50 ng/ml IGF-I, 81 μg/ml peptide or plain DMEM for 30 min at 37°C. Next, cells were lysed in lysis buffer containing 150 mM NaCl, 20 mM Tris pH 7.4, 10% glycerol, 10 mM β-glycerolphosphate, 5 mM tetrasodium pyrophosphate, 1 mM $MgCl_2$, 1 mM $ZnCl_2$ and 1% (v/v) NP-40, phosphatase inhibitors and protease inhibitors, and cleared. The protein concentration in each cell lysate was determined by BCA assay and equal amounts of protein were immunoprecipitated with IGF-IRβ (C-60) antibody and protein A/G agarose. The precipitates were washed three times in washing buffer (20 mM HEPES pH 7.4, 150 mM NaCl, 1 mM EDTA, 1% (v/v) NP-40, 10 mM β-glycerolphosphate, 5 mM tetrasodium pyrophosphate). The samples were run in duplicates in 12 % SDS-polyacrylamide gel electrophoresis (SDS-PAGE), followed by immunoblotting. The blots were blocked in 3 % (w/w) BSA or 5 % (w/w) skim milk, 0.1 % (v/v) Tween-20, 50 mM Tris pH 10.2 and 150 mM NaCl for 30 min, incubated O/N with primary antibody and secondary antibody for two hours. One of the blots was incubated with anti-phosphotyrosine antibody (1:1000 in blocking buffer), the other with IGF-IIRβ antibody (1:200 in blocking buffer). The antibodies were detected using HRP conjugated secondary antibodies (1:1000 in blocking buffer) and enhanced chemiluminescence detection kit. The bands were visualized using the GeneGNOME

and the software GeneTools (Syngene, Cambridge, UK).

4.2.6 Statistics

Statistical analysis of the neurite outgrowth results were performed using one-way analysis of variance (ANOVA) for repeated measurements with the post-test Dunett multiple comparisons test, employing the commercially available software package GraphPad Prism, version 4.03 (GraphPad Software Inc, San Diego, CA, USA). To confirm comparability of the two sets of experiments with different concentration series described in subsection4.2.1, the concentrations common for the two sets were compared using unpaired t-test, again employing the Graphpad Prism, version 4.03. The results are expressed as percentage of the control, where the control corresponds to 100 %, and presented as mean values ± standard error of the mean (S.E.M.). The results are based on at least four independent experiments. The p-values are indicated with asterisks according to following:

$$p < 0.05 = *,\ p < 0.01 = **,\ p < 0.001 = ***$$

Chapter 5

Results

5.1 The induction of neuritogenesis in CGN by IGF-II and IGF-II derived peptides

Neuronal processes, i.e. dendrites and axons, are en masse named neurites and their ability to extend neurites is the first hallmark of differentiation of neurons. The potential of a molecule to induce differentiation of neurons can therefore be evaluated by a neurite outgrowth assay. Here, CGNs from 7-8 days old rats were isolated, incubated with peptides, and the neurite outgrowth was measured. There are several reasons why this type of neurons were used in the assay. CGNs are easy to isolate and yield a relatively high number of cells in the preparation. Moreover, the neuronal culture of cerebellum from 7-8 days old rats consists of 90 % granule cells that have not reached the postmitotic stage of development, but are still capable of differentiate upon stimulation. Additionally, differentiation induced via the IGF-IR is wished to be investigated in this thesis and the IGF-IR has been shown to be expressed in CGN. The cerebellar granular neurons were grown at low density in order to avoid interactions between the cells, as these may complicate the analysis and influence the results. P2d was included as a positive control of the neurons capability of neuritogenesis.

5.1.1 IGF-II derived peptides

CGN were plated on permanox slides and incubated for 24 hours in the presence or absence of peptides at different concentrations. The neurons were immunostained for GAP-43 and the neurite outgrowth was quantified. Several peptides were found to induce neuritogenic responses very effectively. As illustrated in Figures 5.1 and 5.2a, peptide IGF-II-I promotes neurite outgrowth and the maximum effect of 380.4 $\pm$ 48.1 % of the control appears to be at a concentration of 81 μg/ml IGF-II-I. A dose-response study of the neuritogenic effect of this peptide revealed that the induction of neurite

outgrowth is dose-dependent with a bell-shaped curve. The neuritogenic response was statistically significant at concentrations 0.3-81 μg/ml when compared to the control.

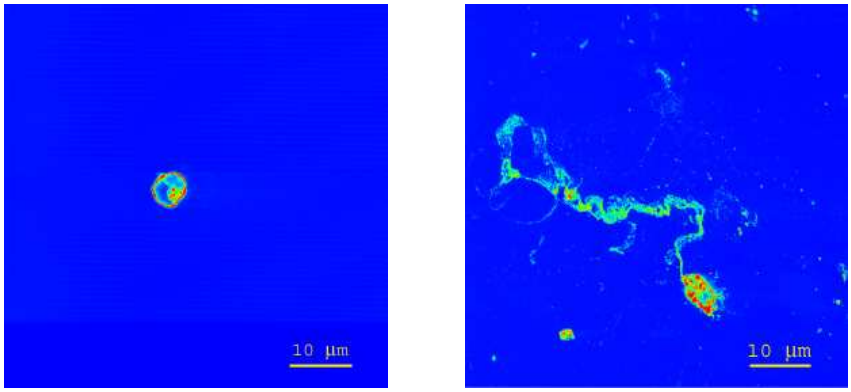

(a) Control (b) 3 μg/ml IGF-II-I

Figure 5.1: Neurite outgrowth induced by IGF-II-I on CGN. CGN from 7-8 days old rats were grown in the presence of 3 μg/ml IGF-II-I peptide or medium alone (control) for 24 hours, followed by fixation and immunostaining with rabbit anti-rat GAP-43 and secondary Alexa Flour 568 goat anti-rabbit antibodies. Images were recorded using a confocal laser connected to a microscope and pseudocolors in the blue-red color scale were applied. (a) CGN treated with medium. (b) CGN treated with 3 μg/ml IGF-II-I. The neurite outgrowth induced by peptides IGF-II type II,III and V exhibited similar morphology. Scale bar: 10μm.

The IGF-II-II also exhibits ability to induce a neuritogenic response, however, with varying response as illustrated by the large SEM relative to the number of experiments (Figure 5.2b). The dose-response study indicates that the neurite outgrowth promoting effect of the peptide is not dose-dependent. Instead, the curve is plateau-shaped as the peptide induces neurite extension at concentrations 0.1 to 243 μg/ml. Although there seems to be an increased effect at the highest concentration used (243 μg/ml) the effect on neurite outgrowth of the IGF-II-II was not evaluated at higher concentrations due to the elevated risk of non-specific binding. Moreover, even though the peptide would be neuritogenic at higher concentrations, it would be of no relevance, since such a high dose is not applicable for practical purposes. Additionally, it was noted in two experiments, that a concentration of 243 μg/ml IGF-II-II resulted in cell death. This implies that 243 μg/ml is a border line concentration, which at low cell density results in cell death, but at higher density cultures, the growth factors synthesized by the surrounding cells have a protective effect and rescues the cells. 9, 81 and 243 μg/ml IGF-II-II stimulated neurite outgrowth, which was statistically significant compared to the control, and their effects were 292.1 $\pm$ 50.8 %, 305.3$\pm$ 83.6 % and 447.2 $\pm$ 105.6 % of the control respectively.

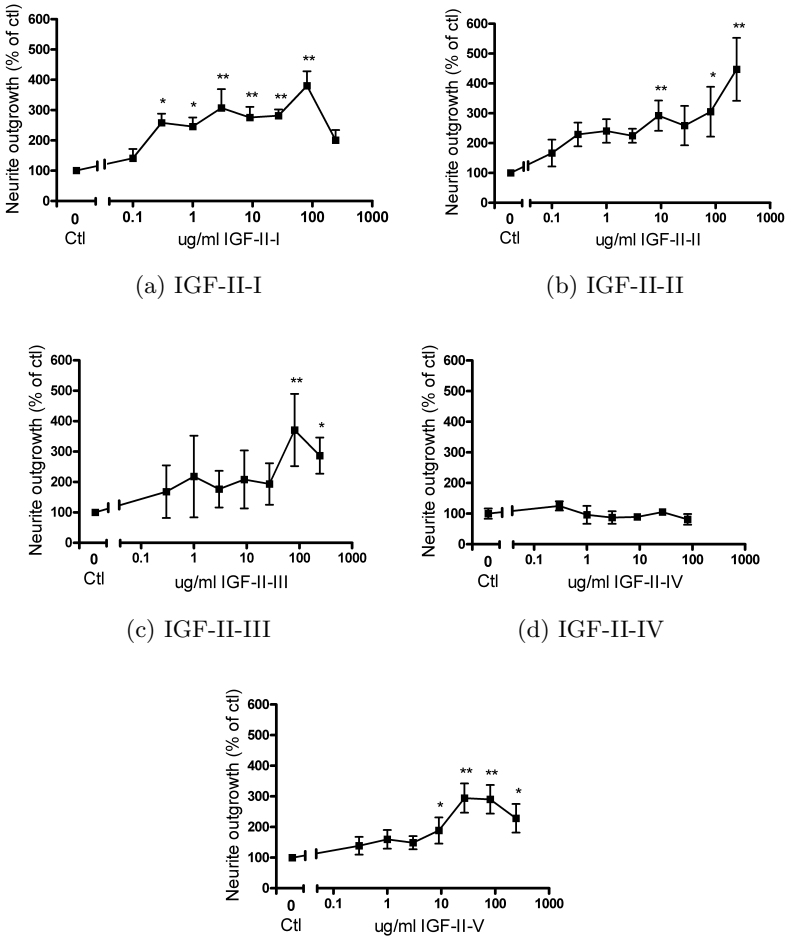

(a) IGF-II-I

(b) IGF-II-II

(c) IGF-II-III

(d) IGF-II-IV

(e) IGF-II-V

Figure 5.2: Neuritogenic effect of IGF-II derived peptides on CGNs. CGNs from 7-8 days old rats were treated with IGF-II derived peptides or medium alone (control) for 24 hours. The average length of neurites for the controls was 16.2 ± 1.3 μm (a) or 17.9 ± 1.6 μm (b) or 19.1 ± 2.2 μm (c) or 28.3 ± 4.7 μm (d) or 19.1 ± 1.5 μm (e). The results are expressed as percentage ± SEM, where the control is set at 100 %. The P2d was used as positive control inducing neurite outgrowth of magnitude 586 ± 62 % (a) or 444 ±185 % (b) or 692 ± 304 % (c) or 254 ± 20 % (d) or 464 ± 98 % (e) of control (data not shown).

The third peptide to be investigated for its neuritogenic potential was IGF-II-III. This peptide stimulates neurite outgrowth, although the effect is most pronounced at higher concentrations. The maximal effect of 370.9 ± 118.6 % of control was observed at 81 μg/ml IGF-II-III. At 81 μg/ml and 243 μg/ml IGF-II-III the neuritogenic effect is statistically significantly different from the outgrowth induced by the media alone. The peptide appears to induce neritogenesis in a dose-dependent manner since there is a tendency of reduced neuritogenic effect at 243 μg/ml compared to 81 μg/ml IGF-II-III (see Figure 5.2c).

As opposed to the previously described peptides, the IGF-II-IV was found not to exhibit any neuritogenic effect on CGNs (Figure 5.2d). Finally, the IGF-II-V was found to induce neurite outgrowth in CGNs. The induction is dose-dependent with an optimal concentration of 27 μg/ml IGF-II-V, resulting in 294.4 ± 47.7 % stimulation compared to the control. The difference between the effect of 9-243 μg/ml IGF-II-V and the control was found to be statistically significant. The fact that IGF-II-IV did not induce neurite outgrowth supports that the effects of the other peptides are specific for each unique peptide. In addition, the fact that the response patterns of the peptides are different also strengthens the specificity of the peptides.

5.1.2 IGF-II

In order to relate the neuritogenic potential of the IGF-II derived peptides to the effect of IGF-II itself, IGF-II was assayed for its ability to induce neuritogenesis. Similarly to the IGF-II derived peptides, CGN were grown for 24 hours in the presence of IGF-II at different concentrations. Due to time limitations, only two experiments were performed (Figure 5.3), and no statistical analysis was done. The results are rather varying, hence no trend in terms of dose-response can be determined. However, the results imply that the efficacy of the growth factor is lower than the neuritogenic effect of the peptides.

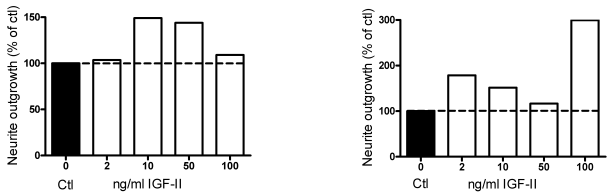

(a) (b)

Figure 5.3: Neuritogenic effect of IGF-II on CGNs. CGNs from 7-8 days old rats were treated with IGF-II (2, 10, 50, 100 ng/ml) or medium alone (control) for 24 hours. The average length of neurites for the controls was 27.5 μm (a) or 21.6 μm (b). The results of two single experiments are shown, where the control is set at 100 %. The P2d was used as positive control inducing neurite outgrowth of magnitude 337 % (a) or 398 % (b) of control (data not shown)

5.2 SPR Analysis

SPR analysis was employed to investigate the binding capability of the peptides for the insulin/IGF family receptors. As the IGF-II binds with different affinities to all receptors, it is of interest to find whether the peptides can mimic the binding of IGF-II to the receptors or not, and if so whether the binding corresponds to a binding site specific for one receptor or common to all.

5.2.1 Preliminary studies on the BIAlite instrument

Preliminary studies of the interaction between the insulin/IGF family receptors and the IGF-II derived peptides were conducted using the BIAlite instrument. The studies were preparative for the subsequent Biacore 2000 studies and the purpose was to give an indication of the binding capabilities of the peptides for the receptors as well as an appreciation of the abilities of the receptors to be immobilized on a sensor chip. The receptors were immobilized on a CM5 sensor chip, one per chip as described in section 4.2.4, and the IGF-II derived peptides were injected over the chip surface at 5 μl/min in HBS-EP buffer. The results (displayed in Figure 5.4) indicate that IGF-II-II and IGF-II-V bind with low affinity to the IGF-IR and with higher affinity to the IGF-IIR and the IR-A. The response of IGF-II-III could correspond to shift in refractive index due to change in molecule density in buffer as the peptide is injected. However, in the IGF-IR and IGF-IIR sensorgrams the IGF-II-III appears to associate to and dissociate from the respective receptors although at very high rate. Thus, binding of the peptide to the IGF-IR and IGF-IIR may exist, but the limited sensitivity of BIAlite hinders the visualization of the rapid binding and release. As peptides IGF-II-I and IGF-II-IV did not demonstrate binding to the receptors even at high

concentration (200 μg/ml, corresponding to 19.8 and 16.3 μM of IGF-II-I and IGF-II-IV respectively) they were considered as non-binding. Since this was a preliminary study, the peptides were only injected once and so, no affinity constants could be calculated.

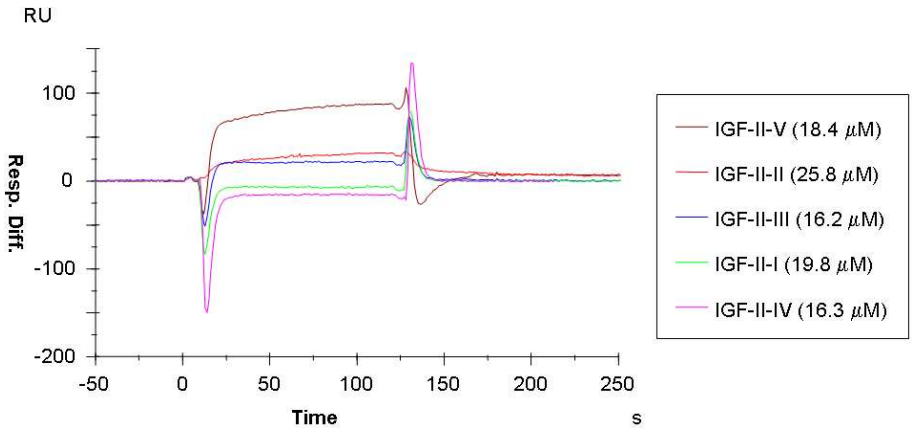

(a) IGF-II derived peptides to IGF-IR.

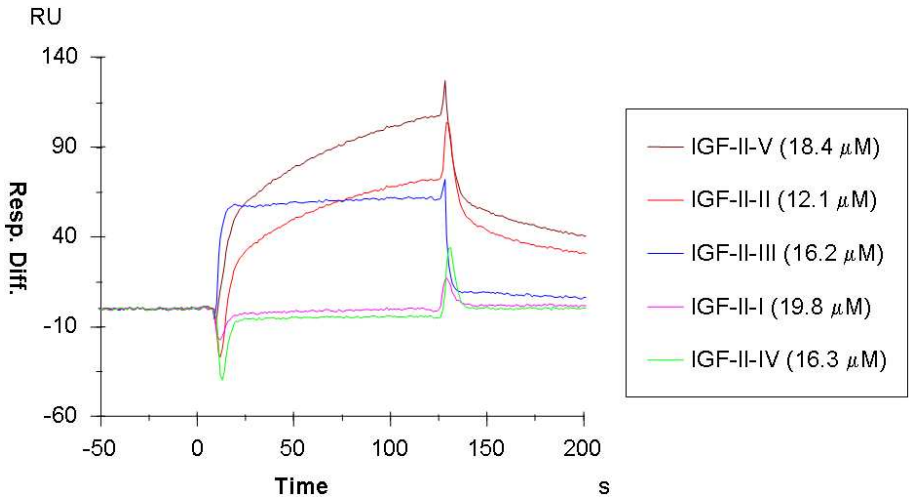

(b) IGF-II derived peptides to IGF-IIR.

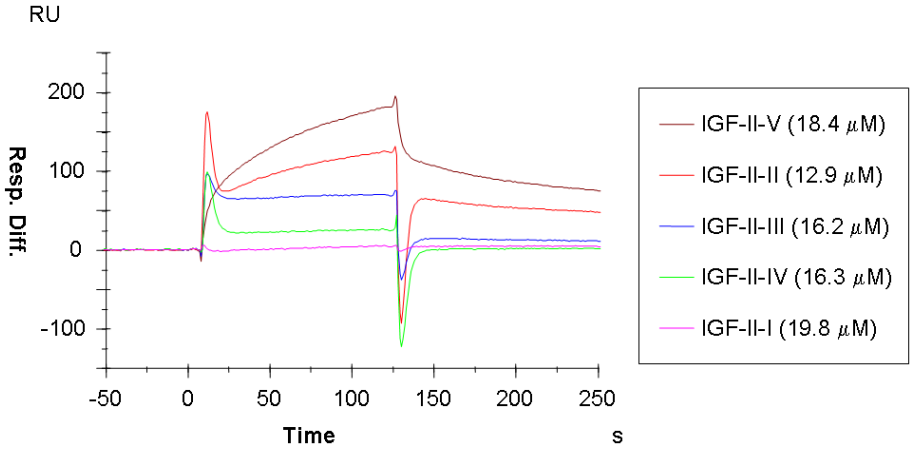

(c) IGF-II derived peptides to IR-A.

Figure 5.4:Preliminary binding studies using the BIAlite instrument. The IGF-IR, IGF-IIR and IR-A were immobilized on separate sensor chips CM5 at densities of 4200, 3200 and 3033 RU, respectively. The binding is expressed in resonance units and corresponds to the difference in binding to the flow cell with immobilized protein and a reference flow cell. Peptides were injected at 5 μl/min in HBS-EP buffer at concentrations indicated in the legend to each sensorgram.

5.2.2 The Biacore 2000

The Biacore 2000 instrument is a newer instrument than the BIAlite and allows for automated analysis of samples. In these studies the receptors were immobilized on a sensor chip CM4, which has a lower degree of carboxymethylation than the CM5, resulting in lower surface charge density. This may reduce eventual non-specific binding of molecules that are positively charged, which is the case for the peptides (pI 10.8-12.6). First, apparent affinity constants for the peptides to the receptors were found. Second, optimization of the interactions between the peptides and receptors was attempted by shifting flow rate. Third, the specificity of the interactions between peptides and receptors was evaluated by studying the interactions between the peptides and a negative control. Finally, in order to assay the performance of the system the affinity constants of the cognate proteins to the receptors were determined and compared to previously calculated affinity constants.

5.2.3 IGF-II derived peptides bind to the insulin/IGF family receptors

IGF-IR, IGF-IIR and IR-A were immobilized on a sensor chip was immobilized as described in section 4.2.4. The peptides were injected in duplicates at 20 μl/min at concentrations 1.6-66 μM in HBS-EP buffer (see Figure 5.5).

Based on these results, apparent affinity constants were calculated using the BIAevaluation software (see Table 5.1). True affinity constants between a monomer and receptor cannot be calculated as the peptides, synthesized as dendrimers, may bind simultaneously to an unknown number of receptors. It should be noted that the results are based on one experiment, i.e. injections over one sensor chip. For convincing results, the experiment should be repeated twice more.

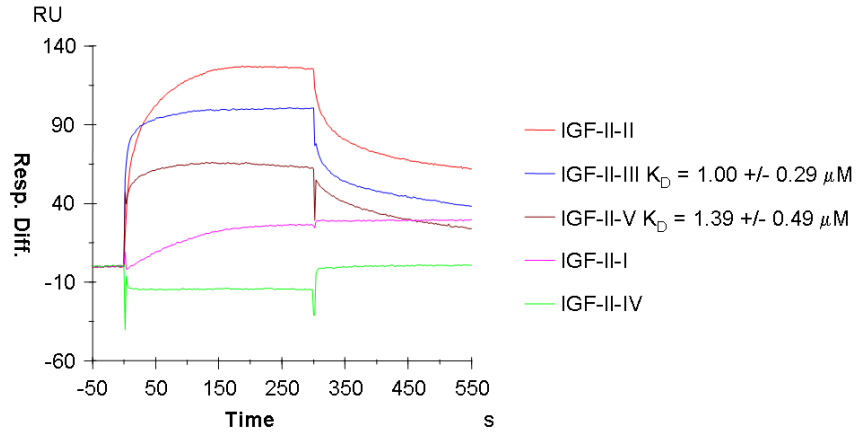

(a) Binding of peptides to the IGF-IR

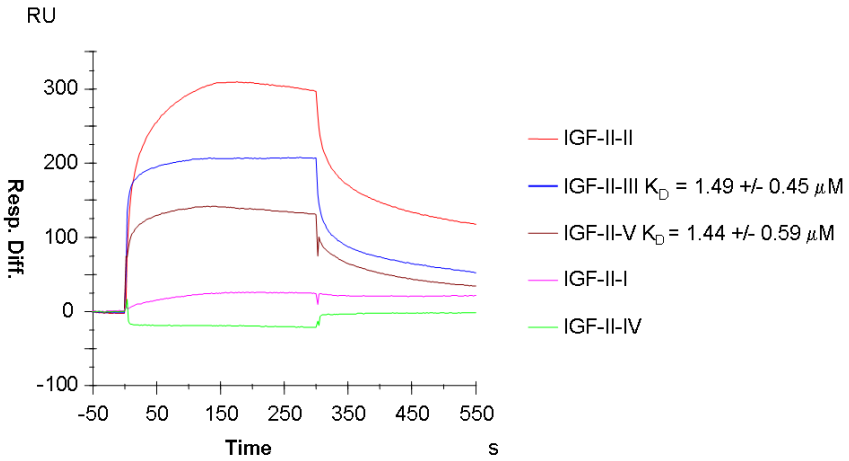

(b) Binding of peptides to the IGF-IIR

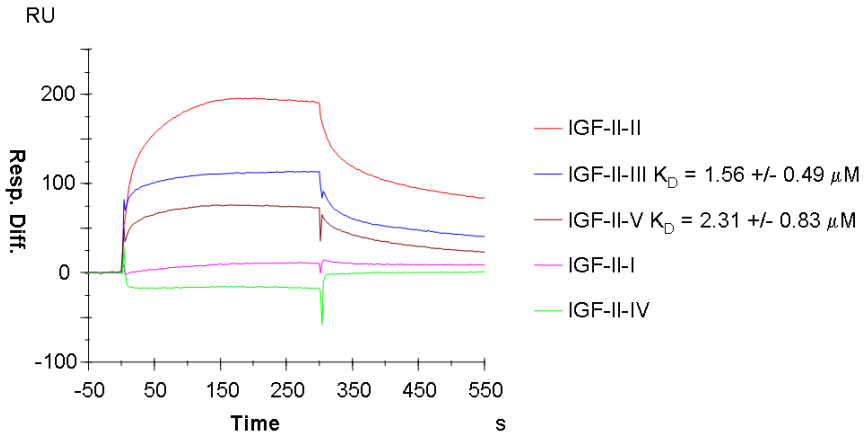

(c) Binding of peptides to the IR-A

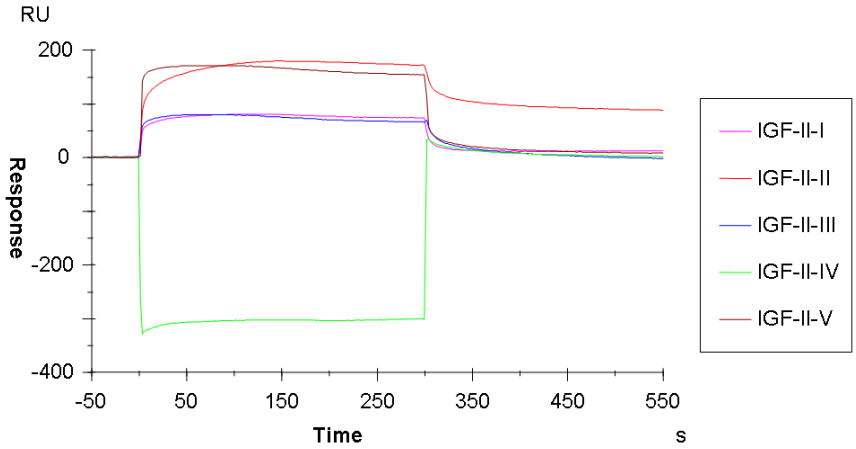

(d) The reference flow cell

Figure 5.5:Binding studies using the Biacore 2000 instrument. The IGF-IR, IGF-IIR and IR-A were immobilized on a sensor chip CM4 to final receptor densities of 1700, 3800 and 2800 RU, respectively. The binding is expressed in resonance units and corresponds to the difference in binding to the flow cell with immobilized protein and a reference flow cell. Based on results from duplicate injections on one sensor chip, the apparent affinity constants were calculated by fitting the curves to a 1:1 Langmuir binding model applying the BIAevalution software. The affinity constants are expressed as means of the K_D of the different concentrations ± SEM, where SEM is calculated from the obtained K_Ds at different concentrations. Representative curves of the peptides at 200 μg/ml are displayed.

Affinity constants: receptors to peptides

	IGF-IR	IGF-IIR	IR (A)
IGF-II-III	1.00 ± 0.29	1.49 ± 0.45	1.56 ± 0.49
IGF-II-V	1.39 ± 0.49	1.44 ± 0.59	2.31 ± 0.62

Table 5.1: Binding affinities of IGF-II-III and IGF-II-V for IGF-IR, IGF-IIR and IR. The affinity constants are expressed in μM. The experiment was performed and affinity constants were calculated as described in Figure 5.2.3.

In agreement with the preliminary studies the IGF-II-V binds to the IGF-IR and the apparent affinity constant was calculated to 1.39±0.49 μM. In addition, the IGF-II-III here displayed binding to the IGF-IR with an affinity constant in a similar range to the other peptide 1.00±0.29 μM. The IGF-II-I does exhibit small association to the IGF-IR when applied at high concentrations (80 μM). However, the response is too small in relation to the response produced by the background (i.e. buffer injection), thus the binding is interpreted as non-existing. The IGF-II-IV did not show any binding to the IGF-IR. Again, the fact that this peptide does not bind, supports the specificity of the other peptides binding to the receptor.

Equally to what was seen for the IGF-IR, IGF-II-III and IGF-II-V binds to the IGF-IIR with apparent affinities ranging from 1.21±0.44 to 1.49±0.45 μM. The IGF-II-I binds in the same way as to the IGF-IR, i.e. yielding a small response at 80 μM that is not possible to distinguish from the response yielded by the buffer injected alone, thus no affinity constant can be calculated. The IGF-II-IV does not exhibit binding to the IGF-IIR. The same peptides that exhibit binding to the IGF-IR ad IGF-IIR also bind to the IR-A with apparent affinity constants of 1.56±0.49 to 2.31±0.83 μM. Again, the IGF-II-I yields only a small response and no affinity constant could be determined. Similarly to the other receptors, IGF-II-VI does not bind to the IR-A.

All peptides injected also pass the reference flow cell, which has an unmodified surface and thus indicates how much of the peptide binding to the flow cell immobilized with receptor is due to non-specific binding, i.e. peptide binding to the dextran surface. Obviously, non-specific binding is unwanted as it complicates the interpretation of the data. The peptides IGF-II type I, III, IV and V do not appear to bind non-specifically to the sensor chip. The responses generated by the injection of these peptides correspond to altered molecule density in the sample compared to the running buffer. This alteration results in a change in refractive index, leading to a response in the sensorgram. The response can be avoided by dissolving the peptides in HBS-EP buffer diluted in water, thereby maintaining the refractive index of the running buffer as the sample is injected.

Conversely, the injection of IGF-II-II results in binding of the peptide to the reference flow cell indicated by association and dissociation of the peptide to the chip. Relative the binding to the IGF-IR the binding to the blank flow cell is approximately 140 % and relative the IR-A and IGF-IIR the binding to the blank is 90 % and 60 %, respectively. Thus, the results from the analysis of the interactions between the IGF-II-II the receptors cannot be used, but they indicate that IGF-II-II bind to the receptors. The interactions of IGF-II-II and receptors could be investigated by reversing

the system, i.e. immobilizing the peptides and injecting the receptors. In general, a low level of binding to the reference cell is permitted as long as the assay performance is not substantially affected.

5.2.4 Optimization of the interaction

In order to obtain a thorough understanding of the interaction between the peptides and the receptors and possibly detect new interactions between peptides and receptors, the analysis was optimized. One mode of optimizing the analysis is by applying different concentrations of the peptides, described previously in section 5.2.3. Furthermore, the binding capability between molecules is influenced by the flow rate. According to the recommendations in the Biacore Sensor Surface Handbook, version AA [2003] the flow rate for kinetic experiments should be >30 μl/min in order to avoid limitations in transport of sample to and from the sensor chip surface. On the contrary, too high flow rate may limit the interactions since the sample passes by more rapidly than the peptide associates to the receptor.

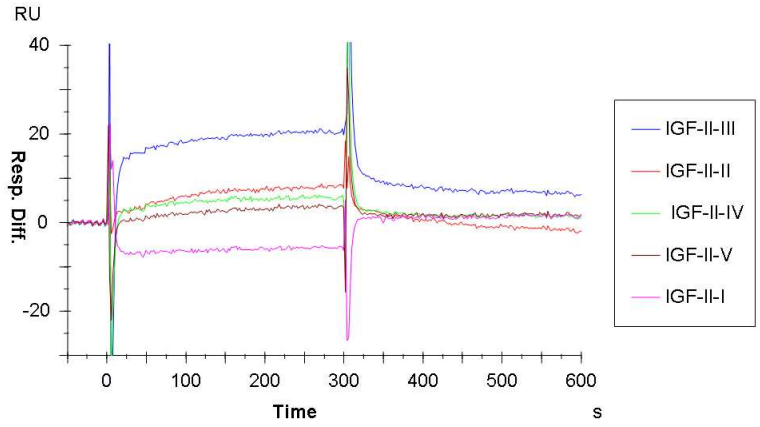

(a) IGF-IR

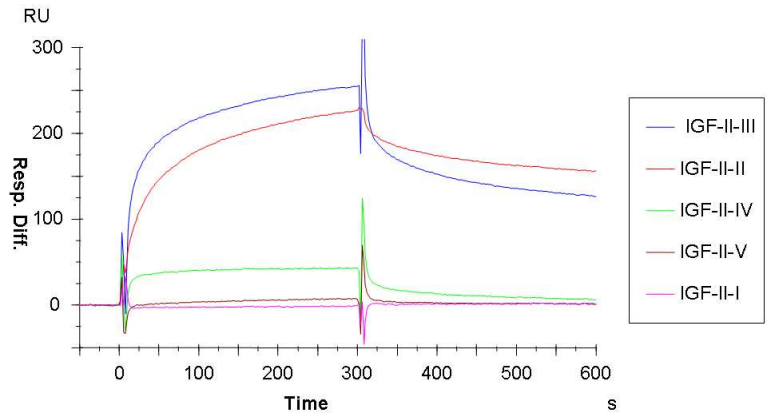

(b) IGF-IIR

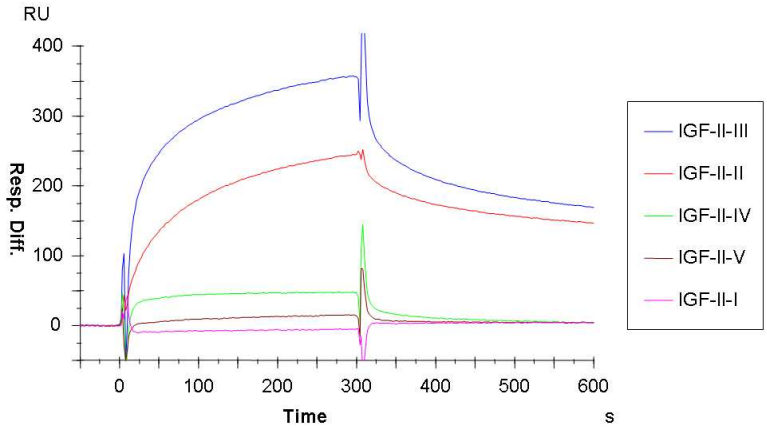

(c) IR-A

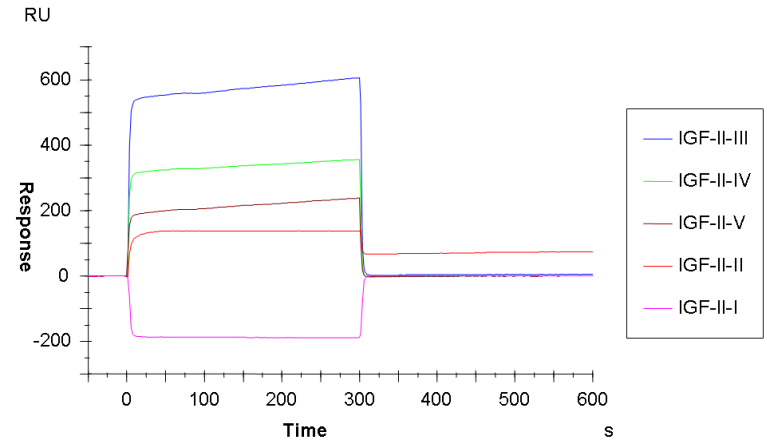

(d) Reference flow cell

Figure 5.6: Binding of peptides at flow rate 5μl/min. IGF-IR, IGF-IIR and IR-A were immobilized on a sensor chip CM4 to a final receptor density of 2577, 2430 and 4664 RU respectively. The binding is expressed in resonance units and corresponds to the difference in binding to the flow cell with immobilized protein and a reference flow cell. Injections of 200 μg/ml peptide in HBS-EP buffer were made at flow rate 5 μl/min.

First the influence of flow rate on interactions was investigated. Analysis of peptide receptor interactions were performed at a flow rate of 5 and 40 μl/min using a peptide concentration of 200 μg/ml (corresponding to 39.6, 25.8, 32.4, 32.7 and 36.8 μg/ml for peptide IGF-II type I-V respectively) in HBS-EP buffer. Due to limited amounts of samples, the peptides were injected once only. At 5 μl/min the binding of peptides to IGF-IR was substantially reduced, only IGF-II-III exhibited binding (see Figure 5.6). All interactions involving IGF-II-V were eliminated, instead slight binding of IGF-II-IV to the IGF-IIR and the IR-A were detected.

At the increased flow rate, 40 μl/min, the IGF-II-I and IGF-II-II bound strongly to the reference cell, which explains the shape of the sensorgrams (see Figure 5.7). The apparent binding of the IGF-II-I to the other receptors is negligible due to the high binding of the peptide to the blank flow cell. Similarly to analysis at 20 μl/min, IGF-II-II binds extensively to the blank flow cell at flow rate of 40 μl/min. In fact, the effect is roughly doubled. Apart from these observations, there were no major differences in the interactions between the peptides and the receptors at high flow rate when compared to 20μl/min.

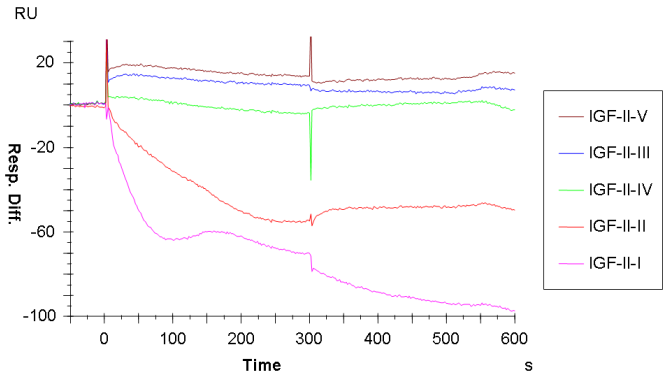

(a) IGF-IR

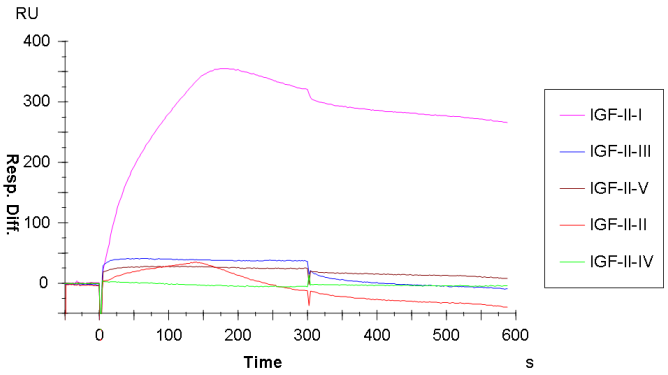

(b) IGF-IIR

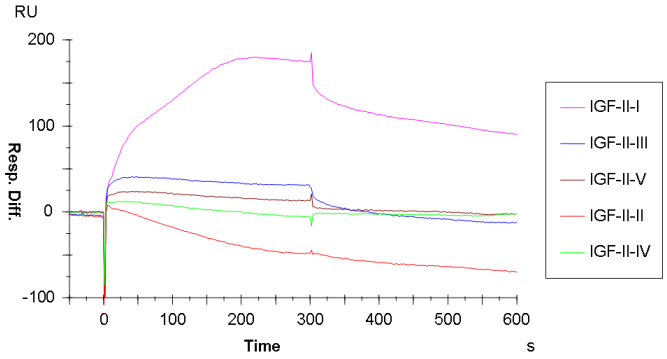

(c) IR-A

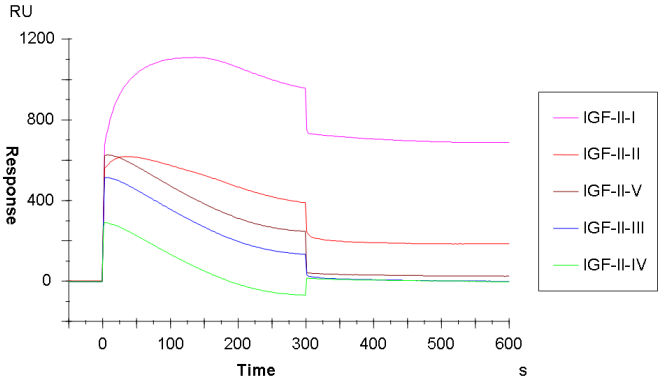

(d) Reference flow cell

Figure 5.7: Binding of peptides at 40μl/min. IGF-IR, IGF-IIR and IR-A were immobilized on a sensor chip CM4 to a final receptor density of 2577, 2430 and 4664 RU respectively. The binding is expressed in resonance units and corresponds to the difference in binding to the flow cell with immobilized protein and a reference flow cell. Injections of 200 μg/ml peptide in HBS-EP buffer were made at flow rate 40 μl/min.

The buffer system also influences the interaction of peptides to receptors. The HBS-EP buffer contains EDTA, a chelating agent that removes metal ions sometimes needed in the binding of a peptide to a receptor. In HBS-EP, the removal of metal ions has an anti-microbial effect and serves to maintain the microbial growth in the instrument as low as possible. In addition, the HBS-EP buffer is advantageous when investigating biological interactions since it is based on HEPES buffer system. This buffer system has maximal buffering capacity at the pH where most biological actions take place, between 6 and 8.

In order to evaluate whether the interaction between peptide and receptor requires Ca^{2+} or Mg^{2+}, SPR analysis can be performed using HBS-P

(without EDTA) supplemented with the metal ions. However, since there has been no reports of metal ions needed for the binding of insulin/IGF family ligands to the receptors, these optimizations were not carried out.

5.2.5 Evaluation of specificity of binding

As the IGF-II type III and V exhibit binding and IGF-II-II indicated to bind to all insulin/IGF family receptors, it is of interest to find a negative control in order to confirm that the binding to the receptors is specific. For this purpose, the peptides were analyzed in duplicates of 200 μg/ml peptide in HBS-EP at 20 μl/min over a sensor chip where the first and second F3 module of NCAM were immobilized (kindly donated by Nikolaj Kulahin). None of the peptides demonstrated binding to the protein (see Figure 5.8).

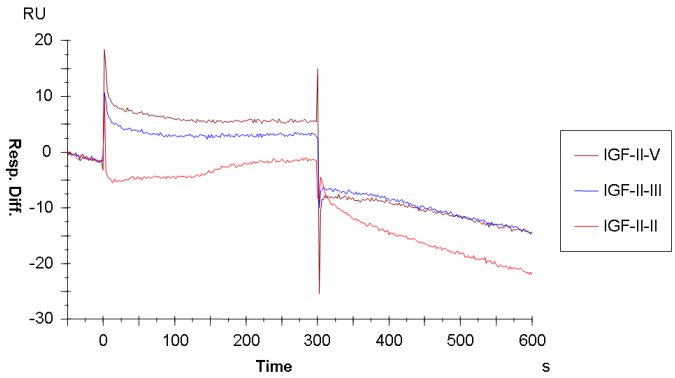

Figure 5.8: Investigation of non-specific binding of peptides. The first and second F3 module of NCAM were immobilized on a sensor chip CM4. The binding is expressed in resonance units and corresponds to the difference in binding to the flow cell with immobilized protein and a blank flow cell. Injections of 200 μg/ml IGF-II-II, IGF-II-III and IGF-II-V in HBS-EP buffer were made at flow rate 20 μl/min.

5.2.6 Verification of the system

In order to validate the results of peptide receptor interactions it is required to verify that the system set up, i.e. the insulin/IGF family receptors immobilized to the sensor chip, is working properly. The affinity constants of the insulin/IGF family ligands to the receptors has been studied extensively as described in section 2.2.1. By analyzing the interactions of the insulin/IGF family ligands to the immobilized receptors affinity constants can be determined. The performance of the system is then evaluated by comparing the K_Ds previously reported with the K_Ds obtained in this study.

IGF-IR, IGF-IIR and IR-A were immobilized on a sensor chip CM4 to a final receptor density of 1200, 2000 and 1600 RU, respectively. The growth factors displayed no binding to the cognate receptors when injected in nM

concentrations, but response was detected when growth factors were used in the μM range. Therefore, the growth factors were injected at 50, 100, 200, 400 and 800 μM and analyzed in HBS-EP at flow rate of 20 μl/min. Insulin was injected in duplicates but the IGF-I and IGF-II were only injected once due to limited amount of each growth factor (see Appendix A for sensorgrams). As a result of the difficulties in fitting the obtained sensorgrams using the BIAevaluation Software, the experimental data was also analyzed as described in section 4.2.4 using Origin v.6.1. The two methods of analyzing sensorgrams generate comparable affinity constants as displayed in Figure 5.9, where the affinity of IGF-I to its cognate receptor was calculated to 13.2 $\pm$3.2 and 11.6 $\pm$3.6 μM using BIAevaluation and Origin v.6.1, respectively.

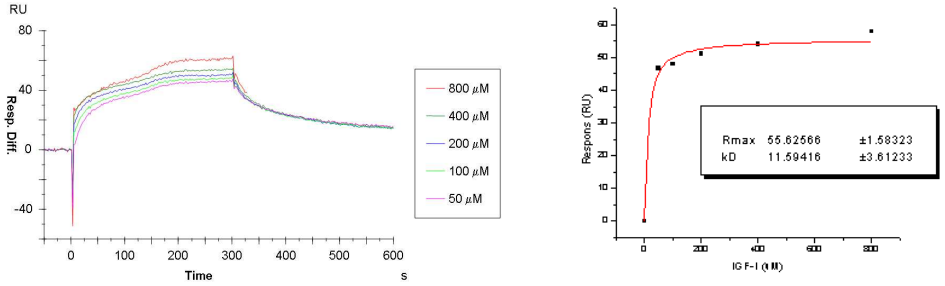

(a) Binding of IGF-I to the IGF-IR

(b) K_D of IGF-I to IGF-IR calculated applying Origin v.6.1

Figure 5.9: IGF-IR affinity for IGF-I determined using two different methods. The IGF-IR was immobilized on a sensor chip CM4 to a final receptor density of 1200 RU. The affinity of IGF-IR for IGF-I was calculated by fitting the curves of IGF-I (a) to a 1:1 Langmuir binding model using BIAevaluation and resulted in a mean K_D value of 13.2 $\pm$ 3.2 μM. The K_D was also calculated from the sensorgrams using the software Origin v.6.1, resulting in a K_D value of 11.6 $\pm$ 3.6 μM (b).

As seen in table 5.2 the K_Ds calculated from experimental data were differing significantly from reported K_D. Thus, these data can not be used to verify the system. Although the experimental K_Ds are much too high, the relative binding of the receptors for IGF-I, IGF-II and insulin appears to be consistent with the reported data, e.g. the IGF-IR binds IGF-I with highest affinity, followed by the IR and last the IGF-IIR.

Affinity constants: receptors to growth factors

IGF-I

	Origin v.6.1	Published data
IGF-IR	11.6 ± 3.6 μM	1 nM
IGF-IIR	407.3 ± 114.7 μM	0.4 μM
IR (A)	63.7 ± 13.8 μM	0.1 μM

IGF-II

	Origin v.6.1	Published data
IGF-IR	42.4 ± 5.7 μM	2-3 nM
IGF-IIR	27.3 ± 10.5 μM	0.2 nM
IR (A)	133.1 ± 42.4 μM	5 nM

Insulin

	Origin v.6.1	Published data
IGF-IR	145.5 ± 30.1 μM	0.1-1 μM
IGF-IIR	-	-
IR (A)	37.5 ± 4.3 μM	0.2-1 nM

Table 5.2: Binding affinities of IGF-I, IGF-II and insulin for IGF-IR, IGF-IIR and IR. By applying the software Origin v.6.1, the experimental K_Ds were calculated from results of single injections of IGF-I and II, and double injections of insulin. The K_Ds are expressed as means of the affinity constants of different concentrations ± SEM. The published K_Ds are collected from Forbes et al. [2002] and Denley et al. [2005a].

5.3 The IGF-IR is potentially phosphorylated by IGF-II derived peptides

Neurite outgrowth analysis indicated activation of the IGF-IR by IGF-II derived peptide I, II, III and V. Moreover, the SPR analysis demonstrated binding between the IGF-IR and IGF-II type III and V, and indicated binding between IGF-IR and IGF-II-II. Based on these results, the ability of the peptides to induce activation of the IGF-IR was determined. Due to time limitations the experiment could only be carried out once and only three peptides were examined: IGF-II, type I, III and V.

HEK293 cells were transiently cotransfected with pEGFP-N_1 and either pCMV6-XL4 containing IGF-IIR cDNA or pcDNA3.1 (empty vector, control). The pEGFP-N_1 encodes GFP and is used as a control of transfection. As the GFP plasmid is transfected in a 1:10 ratio relative the IGF-IR expressing plasmid, its expression will not hinder the expression of IGF-IR. The HEK293 are advantageous in these experiments since the cell line resembles neurons. More specifically, the cell line originates from a neuronal cell in kidney cell cultures and expresses neurofilaments and a variety of

other proteins expressed in neuronal lineage cells [Shaw et al., 2002].

After transfection, the cells were allowed to express the protein for 20 hours, following 30 min stimulation by IGF-I, peptides or nothing. The phosphorylation of the IGF-IR was then determined, following immunoprecipitation and Western blotting. It should be noted that the restricted amount of time allowed no optimization of the experimental set up, instead the method was similar to what has been described previously [Vasilcanu et al., 2006; Kiely et al., 2002; Miyamoto et al., 2004].

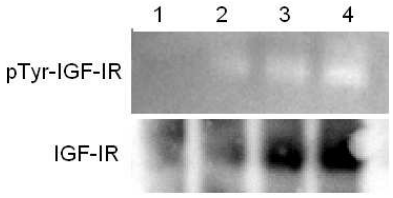

(a) Phosphorylation of IGF-IR in untransfected and transfected HEK293 cells.

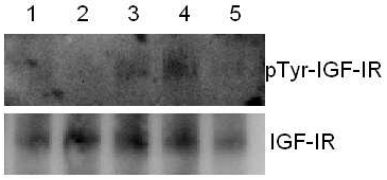

(b) Phosphorylation of IGF-IR induced by IGF-II derived peptides

Figure 5.10: Phosphorylation of the IGF-IR by IGF-II derived peptides. HEK293 were transiently transfected with IGF-IR and incubated with 50 ng/ml IGF-I, 81 μg/ml IGF-II derived peptides or media alone (control) for 30 minutes. Cell lysates were immunoprecipitated for IGF-IR, followed by analysis by Western blotting with antiphosphotyrosine antibodies or anti-IGF-IR. (a) Lane 1 and 2: untransfected, 2 and 4: stimulated with IGF-I.(b) Lane 1: unstimulated, 2: IGF-I 3: IGF-II-I, 4: IGF-II-III, 5: IGF-II-V

Firstly, the necessity of IGF-IR transfection was evaluated by determining the phosphorylation of untransfected and transfected cells, treated with either 50 ng/ml IGF-I or medium alone. The results (Figure 5.10a) indicated that the expression of IGF-IR was of greater magnitude in IGF-IR transfected cells compared to untransfected cells, as would be expected. Furthermore, the phosphorylation of the IGF-IR was more induced both in untransfected cells and IGF-IR transfected cells stimulated with 50 ng/ml IGF-I compared to non-stimulated cells. However, the difference in IGF-IR phosphorylation between stimulated and non-stimulated cells appeared larger in the IGF-IR transfected cells. Since the endogenously expressed IGF-IR in HEK293 cells is not sufficient for detecting differences in IGF-IR phosphorylation between stimulated and non-stimulated cells, the cells in the subsequent experiment were transfected with IGF-IR. Also, in order to decrease the background of IGF-IR phosphorylation, cells were starved for six hours before stimulation with 50 ng/ml IGF-I (positive control), 81 μg/ml peptides or media alone (negative control) for 30 min.

As seen in Figure 5.10b phosphorylation of IGF-IR was not detected in

any of the controls. However, there is a vague detection of phosphorylation in cells treated with IGF-II-III and perhaps also in the cells treated with IGF-II-I. The results are not very convincing, especially since the positive control did not work properly, but they may point towards a possible effect of IGF-II-III and IGF-II-I on IGF-IR activation.

5.4 Summary of results

The results are summarized in Table 5.3, also including a comparison with the growth factors IGF-I, IGF-II and insulin.

	N.O.	IGF-IR	IGF-IIR	IR	IGF-IR Phos
Peptides					
IGF-II-I	Yes	-	-	-	Slight
IGF-II-II	Yes	-	-	-	N.A.
IGF-II-III	Yes	1.00 μM	1.49 μM	1.56 μM	Yes
IGF-II-VI	No	-	Low	Low	N.A.
IGF-II-V	Yes	1.39 μM	1.44 μM	2.31 μM	No
Growth factors					
IGF-I	N.A.	1 nM	0.4 μM	0.1 μM	Yes
IGF-II	Yes	2-3 nM	0.2 nM	5 nM	Yes
Insulin	N.A.	0.1-1 μM	-	0.2-1 nM	Yes

Table 5.3: Summary of the results obtained from neurite outgrowth assay (N.O.), SPR analysis and IGF-IR phosphorylation assay. The affinity constants of IGF-IIR and IR for IGF-II-IV were not calculated as only one experiment was carried out at 5 μl/min. Peptides IGF-II and IGF-IV were not examined in the IGF-IR phosphorylation assay, i.e. not applicable (N.A.). Also, IGF-I and insulin have not been examined for their neuritogenic effect on CGNs, neither in these nor previously published studies.

Chapter 6

Discussion

6.1 Neuritogenesis induced by IGF-II derived peptides

The ability of the IGF-II derived peptides to induce differentiation in CGNs was investigated in a neurite outgrowth assay, a rather simple assay with advantages as well as disadvantages. As the only factor, which can affect neuritogenesis, is the stimulus added to the culture, the assay allows investigations of the capacity of a particular substance to induce neuronal differentiation via the endogenously expressed receptors. On the other hand, the method delivers a very rough estimation of the neuritogenic effect of the molecule *in vivo*, and it does not make allowance for molecules that require binding to the extracellular matrix to be able to bind properly to their receptors.

Four of the peptides (all except for IGF-II-IV) were found to induce neurite outgrowth with a similar maximal effect (approximately 300-400 % of control) although at different concentrations. IGF-II-I and IGF-II-II promote neurite outgrowth at a greater range of concentrations than IGF-II-III and IGF-II-V, which are required in slightly higher concentrations to yield a significant effect. Altogether, these peptides mimick the effect of the IGF-II. The investigations of the neuritogenic effect of the IGF-II were limited but gave an indication of a reduced efficacy relative to the peptides. However, these results cannot be confirmed given that the neuritogenic effect of this growth factor does not appear to have been reported previously.

The seeming difference in neuritogenic effect between the growth factor and the peptides can be explained by the complex interaction between the IGF-II and IGF-IR compared to the peptide IGF-IR interaction. More specifically, the three-dimensional structure of a protein is of significance for the binding of the protein since it determines the positioning of the binding sites,

ensuring they are in the optimal arrangement for binding. Nevertheless, when maintaining the binding sites in the optimal conformation, the tertiary structure may also cause steric hindrance resulting in reduced binding of the growth factor to its receptor. For example, it has been suggested that the C domain of the IGFs cause decreased access to the IR by steric interference, explaining the low affinity of the IR for IGF-II compared to insulin, which does not contain a C domain [Denley et al., 2004]. Peptides only exhibit secondary structure and thereby the risk of steric hindrance and inadequately presented binding sites is avoided.

The fact that many proteins rely on interaction between several sites to activate the receptor is another reason why peptides may yield greater effect than the cognate proteins. One site may correspond to the specificity of the binding, while another site controls receptor activation. For instance, IGF-II C domain has been hypothesized to determine the specificity of the IR and the IGF-IR binding not only by sterical means as stated above, but also by certain residues (no data available of the role of the C domain in IGF-IIR binding)[Denley et al., 2005a]. Thus, the C domain could putatively regulate the specificity of the receptor binding (IGF-IR or IR), and the A and B domains activate the receptor without specificity for the kind of insulin/IGF family receptor. If the peptides contain the receptor activating binding site but not the site regulating receptor specificity, they could potentially bind and activate the IR, IGF-IR and the IGF-IIR with higher efficiency. This could possibly yield a greater effect on survival, proliferation and differentiation of neurons than the growth factor would produce. Moreover, a protein carries modulating regions, i.e. binding sites that mediate opposing effects of the receptor activating binding sites and thereby regulate the total effect of the protein. Since these regions are most likely not in peptides, the activity of the peptide is not counteracted and by these means the peptide may have greater effect on receptor activation than the protein. Finally, since the peptides are synthesized as tetrameric dendrimers, they may activate two receptors simultaneously and thus result in a greater response than the corresponding protein which only activates one receptor at a time.

As mentioned above, the peptides may be less specific in their binding to receptors than the cognate protein and non-specific binding may be the cause of the increased effect on neurite outgrowth. The specificity of the peptides can be evaluated by applying scrambled peptides or inhibitors to the neurite outgrowth assay. More precisely, the decreased effect of the peptides when used in combination with inhibitors for the IGF-IR would ensure that the effect of the peptides is mediated through the IGF-IR. Furthermore, to get a more complete picture of the signaling pathway activated by the peptides, the effect of inhibitors of Erk MAPKK or PI3 kinase on peptide induced neu-

rite outgrowth could be studied. The other mode of investigating whether the neuritogenic activity of the peptides depends on IGF-IR activation is to study neuritogenic potential of scrambled peptides, which consist of amino acids from the same region as the peptide only in a different, randomly chosen arrangement. Additionally, the binding of the peptides to the IGF-IR can be characterized by making alanine substitutions of particular residues of the peptide and study the change in neuritogenic activity. These investigations would be of interest to carry out on the IGF-II derived peptides I, II, III and V.

6.2 Binding of the IGF-II derived peptides to the insulin/IGF receptors

The apparent affinity constants of the peptides for the receptors were calculated by fitting the sensorgrams to a 1:1 Langmuir binding model, which describes the interaction between two molecules as the binding between the growth factors and the receptors. However, the peptides do not necessarily bind according to this model since they are synthesized as tetrameric dendrimers. This means that the peptides sometimes interact 1:1 with the receptors and sometimes the peptides behave divalently, binding to two receptors simultaneously. This behavior is sometimes noted in the equilibrium phase of the interaction, which should be plateau-like, but instead the sensorgram is increasing as seen in the behavior of IGF-II-II and IGF-II-III in Figure 5.2.4. Even though the fitting model is not ideal, it was acceptable as it fitted satisfactory to the association and dissociation phases. The problem with fitting may be solved by reversing the system (i.e. by immobilizing peptide to the sensor chip and injecting the receptors) or using peptides synthesized as dimeric dendrimers.

The SPR analysis revealed binding between the IGF-II derived peptides type III and V and all receptors of the insulin/IGF family, i.e. the peptides mimic the IGF-II in its binding. However, as opposed to the varying affinity of the IGF-II to the IR, IGF-IR and IGF-IIR, the bindings between peptides and the receptors were of similar apparent affinities, ranging from 1.0 to 2.3 μM. The similarity in binding affinity suggests that the peptides contain binding sites of the IGF-II that are common for all three receptors. There have been few studies on the binding sites of IGF-II to the respective receptors, but the existing investigations based on mutations of IGF-II and its ability to bind receptors, show that residues in the B domain of the growth factor (B26 and B27) as well as in the A domain (Val43) are important sites for the binding to both IGF-IR and IR. The mutations of B26 and B27 slightly affect the affinity of IGF-IIR to the IGF-II, but the impact of Val43 in the IGF-II A domain on IGF-IIR affinity has not been investigated [Roth

et al., 1991; Sakano et al., 1991]. Altogether, the reported data support the theory of common binding sites in the IGF-II for the three receptors. The location of the determined binding sites from this study (corresponding to the peptides) cannot be further compared to reported data as the sequences of the peptides are not patented to date. The biological impact of the peptides binding without discrimination to all receptors would potentially be that the IGF-II-III and -V also mimic the IGF-II in its activation of IR-A. Since IGF-II signaling via the IR leads to upregulation of genes involved in protection from apoptosis and has been shown to promote cell survival *in vivo*, the effects of the peptides could be further investigated in an assay of neuronal survival.

The fact that the interactions between IGF-II-III and receptors were not detected in the preliminary studies using the BIAlite is not surprising since the instrument, being older than the Biacore 2000, is not as sensitive as the Biacore 2000, and the flow rate applied in the investigations was rather low, 5 μl/min. As shown in the optimizing experiments, low flow rate limits the binding of the IGF-II-III as well as the IGF-II-V. This is explained by mass transfer limitations. More precisely, interaction between two molecules is determined by the rate of biochemical interaction and the rate of mass transport. Therefore, if the interaction is fast and the transport of peptides is slow, the interaction is limited by the transport of peptide to site of interaction. In order to obtain the optimal conditions for analysis, the flow rate should not hinder the interaction, as the flow rate apparently does at 5 μl/min. The specificity of the interactions was verified when the IGF-II type II, III and V were injected over a chip containing modules 1 and 2 of NCAM F3, without displaying any interactions.

The binding of IGF-II-III, -V and potentially -II to the receptors is consistent with the findings of the neuritogenic potential of the same peptides. Surprisingly, there was initially no detectable interaction between the IGF-II-I and the IGF-IR in the binding studies. Interaction would be expected since the peptide displayed neuritogenic activity in the neurite outgrowth assay with an efficacy similar to that of IGF-II type II, III and V. Similar to these peptides, the interaction between the IGF-II-I and receptors appears to be limited by mass transfer since the binding is drastically increased when the peptide is injected over the flow cell at a higher flow rate (40 μl/min in HBS-EP). However, at this high flow rate the peptide also binds strongly to the reference flow cell, making it is difficult to conclude whether the binding is specific for the receptors. Likewise, the non-specific binding of the IGF-II-II was increased when injected at a higher flow rate. The non-specific binding of IGF-II type I and II to the dextran surface may be overcome by adding Non-Specific Binding (NSB) reducer (Biacore AB, Uppsala, Sweden) to the samples. This would give a better appreciation of the binding of

the IGF-II-I and IGF-II-II to the receptors. Alternatively, the system can be reversed to avoid the disturbance of non-specific binding. The resulting apparent affinity constant from this system ought to be identical to the apparent K_D value obtained from experiments employing the other system. Accordingly, it would be of interest to reverse the system for all peptides to verify the obtained apparent K_D values. Yet another solution to non-specific binding problems is to increase the ionic strength of the buffer. The HBS-EP has low ionic strength (150 mM) and non-specific binding caused by electrostatic interactions may be reduced with buffer containing higher salt concentration [Biacore Sensor Surface Handbook, version AA, 2003].

Contrary to the other peptides, a minor binding of the IGF-II-IV to the IGF-IIR and the IR-A was obtained when the flow rate was decreased to 5 μl/min (HBS-EP). Again, mass transfer is a probable explanation, only here the slow interaction is limited by the high rate of the flow. Similarly to the IGF-II-II, -III and -V , the impact of the peptide binding to the IR could potentially be investigated in an assay of neuronal survival, which is suggested to be mediated through the IR upon IGF-II binding. The peptide did not have any neuritogenic effect, which is consistent with the results obtained in the binding experiments.

The affinity constants obtained by analyzing the interactions of insulin, IGF-I and IGF-II to the IR, IGF-IR and IGF-IIR did not agree with previously reported affinity constants, thus the system could not be verified. The growth factors should exhibit binding to their cognate receptors at nM concentrations, but in these studies interactions were first detected at μM concentrations of the factors. Certainly, the poor affinity could be due to malfunctioning receptors immobilized on the chip. However, since the peptides exhibited such high and specific affinity to the receptors it is more likely that impurity or degradation of the growth factors resulting in lower concentration is the reason for the poor analysis. Another influencing factor may be the density of receptors immobilized on the sensor chip. The amount of receptors immobilized was approximately 30-40 % less than the density of receptors immobilized in previous experiments, which may have led to decreased binding capacity of growth factors. Therefore, growth factors purchased from another supplier will be analyzed in the same system, where the sensor chip will have receptors immobilized at the approximately same density as in former experiments.

6.3 IGF-IR phosphorylation

The IGF-II derived peptides III and possibly I were indicated to activate the IGF-IR, which would be in line with the ability of IGF-II-III to bind to the

IGF-IR and the capacity of both peptides to induce neuronal differentiation. Clearly, the results are very limited, both quantitatively and qualitatively. Thus, optimization of the experimental set up in terms of time and concentration of peptide stimulation and the ideal immunoprecipitation mode (IGF-IR, alternatively phosphotyrosine) is required in future studies. Subsequently, more experiments, including also the IGF-II-II and the cognate protein IGF-II, would give a better understanding the ability of the peptides to mimic the IGF-II induced activation of IGF-IIR.

Chapter 7

Conclusion and perspectives

Two IGF-IR binding sites in IGF-II have been characterized using IGF-II derived peptides. The binding sites, corresponding to the IGF-II derived peptides III and V, are believed to be common for all three receptors of the insulin/IGF family and lead to binding without discrimination, as indicated by the similar apparent affinity constants. The same peptides induced neuronal differentiation and one of them (IGF-II-III) showed indications of activating the IGF-IR. The IGF-II-II exhibits neuritogenic effects and potentially binds to the receptors, thus this peptide may correspond to yet another binding site in IGF-II to all three receptors. Also the IGF-II-I peptide mimics the IGF-II ability to induce neurite outgrowth, however, the binding analysis did not detect any binding to the IGF-IR or its fellow insulin/IGF receptor members. The IGF-II-IV was shown to interact to some extent with the IR and the IGF-IIR, i.e. the peptide may correspond to a IR and IGF-IIR specific binding site of the IGF-II. In agreement with the binding studies the peptide does not have a neuritogenic effect. This is in line with the neuritogenic responses being mediated through the IGF-IR.

For the future, it would be of interest to employ SPR analysis for further investigations of the interactions between the IGF-II derived peptides and the insulin/IGF receptors. Specifically, this could elucidate how the IGF-II-I mediates the neuritogenic effects and, by reversing the system, the apparent affinity constant of the receptors to IGF-II-II could be obtained. In addition, the apparent affinity constants determined in this study for the insulin/IGF receptors to the IGF-II derived peptides could be confirmed. Furthermore, by subjecting the peptides to competitive assays, the picture of the peptide receptor interaction would become more complete.

Regarding the neurite outgrowth assay, it would be valuable to verify that the detected effect is mediated through the IGF-IR, and to investigate which signaling pathways are activated by receptor stimulation. Such studies

would indicate for example whether the different activating binding sites are specific for particular signaling pathways. Additionally, IGF-II has been suggested to play a role in neuroprotection and this could potentially be mimicked by the peptides, hence it would be preferable to examine their effect in a neuronal survival assay. Since the binding experiments have suggested that four of the peptides also exhibit binding to the IR-A, it would be interesting to study the capacity of the peptides to mimic IGF-II induced activation of the IR-A, and subsequent promotion of survival, proliferation and migration. More specifically, this could be done by receptor activation studies and survival studies using inhibitors for different signaling molecules of the IR signaling pathways.

Besides clarifying the structure function relationship of the IGF-II to the insulin/IGF receptors, the IGF-II peptide mimetics could play a role in the research of a therapeutic rescue for several neurodegenerative disorders. As discussed in the section 2.3, IGF-I, IGF-II and insulin sensitizers could have an impact on diseases characterized by insulin and IGF-I resistance. IGF-II mimetic peptides could potentially function as IGF-II agonists for this purpose. Moreover, the finding of IGF-II binding sites for IR-A opens up another field of therapeutic research, namely therapeutic cancer research. The expression and signaling of IGF-II via the IR-A has been found to be upregulated in cancer tissue, why it has been suggested that the IR-A plays a role in cancer [Denley et al., 2003]. If the IR-A binding peptides have antagonistic qualities, they may serve as therapeutic tool in cancer treatment.

Acknowledgements

I am very grateful to Elisabeth Bock and Vladimir Berezin for giving me the opportunity of working in their laboratory and for always being very helpful, guiding and enthusiastic about the work. In addition I would like to acknowledge Lene Køhler and Gro Klitgaard Povlsen for introducing me to cell culture work and Claus Christensen for all his help with the binding studies. Also, I wish to thank all fellow colleagues at Protein laboratory for answering questions and helping out in the laboratory, especially Janne Nielsen and Kamil Gotfryd for proofreading the manuscript. Finally, I would like to thank my reviewer Dan Lindholm for his comments and suggestions.

Bibliography

Baker, E. N., Blundell, T. L., Cutfield, J. F., Cutfield, S. M., Dodson, E. J., Dodson, G. G., Hodgkin, D. M., Hubbard, R. E., Isaacs, N. W., and Reynolds, C. D. (1988). The structure of 2Zn pig insulin crystals at 1.5 A resolution. *Philos Trans R Soc Lond B Biol Sci*, 319(1195):369–456.

Beilharz, E. J., Bassett, N. S., Sirimanne, E. S., Williams, C. E., and Gluckman, P. D. (1995). Insulin-like growth factor II is induced during wound repair following hypoxic-ischemic injury in the developing rat brain. *Brain Res Mol Brain Res*, 29(1):81–91.

Bell, G. I., Pictet, R. L., Rutter, W. J., Cordell, B., Tischer, E., and Goodman, H. M. (1980). Sequence of the human insulin gene. *Nature*, 284(5751):26–32.

Berezin, V. and Bock, E. (2004). NCAM mimetic peptides: Pharmacological and therapeutic potential. *J Mol Neurosci*, 22(1-2):33–39.

Biacore Sensor Surface Handbook, version AA (2003).

Blakesley, V. A., Scrimgeour, A., Esposito, D., and Le Roith, D. (1996). Signaling via the insulin-like growth factor-I receptor: does it differ from insulin receptor signaling? *Cytokine Growth Factor Rev*, 7(2):153–159.

Blundell, T. L., Dodson, G. G., Dodson, E., Hodgkin, D. C., and Vijayan, M. (1971). X-ray analysis and the structure of insulin. *Recent Prog Horm Res*, 27:1–40.

Bondy, C. A. and Cheng, C. M. (2004). Signaling by insulin-like growth factor 1 in brain. *Eur J Pharmacol*, 490(1-3):25–31.

Brissenden, J. E., Ullrich, A., and Francke, U. (1984). Human chromosomal mapping of genes for insulin-like growth factors I and II and epidermal growth factor. *Nature*, 310(5980):781–784.

Chen, H.-K., Fernandez-Funez, P., Acevedo, S. F., Lam, Y. C., Kaytor, M. D., Fernandez, M. H., Aitken, A., Skoulakis, E. M. C., Orr, H. T., Botas, J., and Zoghbi, H. Y. (2003). Interaction of Akt-phosphorylated ataxin-1 with 14-3-3 mediates neurodegeneration in spinocerebellar ataxia type 1. *Cell*, 113(4):457–468.

Chrysis, D., Calikoglu, A. S., Ye, P., and D'Ercole, A. J. (2001). Insulin-like growth factor-I overexpression attenuates cerebellar apoptosis by altering the expression of Bcl family proteins in a developmentally specific manner. *J Neurosci*, 21(5):1481–1489.

Daughaday, W. H., Hall, K., Raben, M. S., Salmon, W. D. J., van den Brande, J. L., and van Wyk, J. J. (1972). Somatomedin: proposed designation for sulphation factor. *Nature*, 235(5333):107.

de la Monte, S. M. and Wands, J. R. (2005). Review of insulin and insulin-like growth factor expression, signaling, and malfunction in the central nervous system: relevance to Alzheimer's disease. *J Alzheimers Dis*, 7(1):45–61.

De Meyts, P. (1994). The structural basis of insulin and insulin-like growth factor-I receptor binding and negative co-operativity, and its relevance to mitogenic versus metabolic signalling. *Diabetologia*, 37 Suppl 2:135–148. Biography.

De Meyts, P., Christoffersen, C. T., Urso, B., Wallach, B., Gronskov, K., Yakushiji, F., and Shymko, R. M. (1995). Role of the time factor in signaling specificity: application to mitogenic and metabolic signaling by the insulin and insulin-like growth factor-I receptor tyrosine kinases. *Metabolism*, 44(10 Suppl 4):2–11.

Delaney, C. L., Russell, J. W., Cheng, H. L., and Feldman, E. L. (2001). Insulin-like growth factor-I and over-expression of Bcl-xL prevent glucose-mediated apoptosis in Schwann cells. *J Neuropathol Exp Neurol*, 60(2):147–160.

Denley, A., Bonython, E. R., Booker, G. W., Cosgrove, L. J., Forbes, B. E., Ward, C. W., and Wallace, J. C. (2004). Structural determinants for high-affinity binding of insulin-like growth factor II to insulin receptor (IR)-A, the exon 11 minus isoform of the IR. *Mol Endocrinol*, 18(10):2502–2512.

Denley, A., Cosgrove, L. J., Booker, G. W., Wallace, J. C., and Forbes, B. E. (2005a). Molecular interactions of the IGF system. *Cytokine Growth Factor Rev*, 16(4-5):421–439.

Denley, A., Wallace, J. C., Cosgrove, L. J., and Forbes, B. E. (2003). The insulin receptor isoform exon 11- (IR-A) in cancer and other diseases: a review. *Horm Metab Res*, 35(11-12):778–785.

Denley, A., Wang, C. C., McNeil, K. A., Walenkamp, M. J. E., van Duyvenvoorde, H., Wit, J. M., Wallace, J. C., Norton, R. S., Karperien, M., and Forbes, B. E. (2005b). Structural and functional characteristics of the Val44Met insulin-like growth factor I missense mutation: correlation with effects on growth and development. *Mol Endocrinol*, 19(3):711–721.

D'Ercole, A. J., Ye, P., Calikoglu, A. S., and Gutierrez-Ospina, G. (1996a). The role of the insulin-like growth factors in the central nervous system. *Mol Neurobiol*, 13(3):227–255.

D'Ercole, A. J., Ye, P., and Gutierrez-Ospina, G. (1996b). Use of transgenic mice for understanding the physiology of insulin-like growth factors. *Horm Res*, 45 Suppl 1:5–7.

Derewenda, U., Derewenda, Z., Dodson, G. G., Hubbard, R. E., and Korber, F. (1989). Molecular structure of insulin: the insulin monomer and its assembly. *Br Med Bull*, 45(1):4–18.

Dodson, G. and Steiner, D. (1998). The role of assembly in insulin's biosynthesis. *Curr Opin Struct Biol*, 8(2):189–194.

Du, Y. C., Zhang, Y. S., Lu, Z. X., and Tsou, C. L. (1961). Resynthesis of insulin from its glycyl and phenylalanyl chains. *Sci Sin*, 10:84–104.

Dudek, H., Datta, S. R., Franke, T. F., Birnbaum, M. J., Yao, R., Cooper, G. M., Segal, R. A., Kaplan, D. R., and Greenberg, M. E. (1997). Regulation of neuronal survival by the serine-threonine protein kinase Akt. *Science*, 275(5300):661–665.

Ebina, Y., Ellis, L., Jarnagin, K., Edery, M., Graf, L., Clauser, E., Ou, J. H., Masiarz, F., Kan, Y. W., and Goldfine, I. D. (1985). The human insulin receptor cDNA: the structural basis for hormone-activated transmembrane signalling. *Cell*, 40(4):747–758.

Forbes, B. E., Hartfield, P. J., McNeil, K. A., Surinya, K. H., Milner, S. J., Cosgrove, L. J., and Wallace, J. C. (2002). Characteristics of binding of insulin-like growth factor (IGF)-I and IGF-II analogues to the type 1 IGF receptor determined by BIAcore analysis. *Eur J Biochem*, 269(3):961–968.

Froesch, E. R., Muller, W. A., Burgi, H., Waldvogel, M., and Labhart, A. (1966). Non-suppressible insulin-like activity of human serum. II. Biological properties of plasma extracts with non-suppressible insulin-like activity. *Biochim Biophys Acta*, 121(2):360–374.

Gerozissis, K. (2003). Brain insulin: regulation, mechanisms of action and functions. *Cell Mol Neurobiol*, 23(1):1–25.

Giovannone, B., Scaldaferri, M. L., Federici, M., Porzio, O., Lauro, D., Fusco, A., Sbraccia, P., Borboni, P., Lauro, R., and Sesti, G. (2000). Insulin receptor substrate (IRS) transduction system: distinct and overlapping signaling potential. *Diabetes Metab Res Rev*, 16(6):434–441.

Guan, J., Bennet, L., Gluckman, P. D., and Gunn, A. J. (2003). Insulin-like growth factor-1 and post-ischemic brain injury. *Prog Neurobiol*, 70(6):443–462.

Harper, M. E., Ullrich, A., and Saunders, G. F. (1981). Localization of the human insulin gene to the distal end of the short arm of chromosome 11. *Proc Natl Acad Sci U S A*, 78(7):4458–4460.

Humbel, R. E. (1990). Insulin-like growth factors I and II. *Eur J Biochem*, 190(3):445–462.

Humbert, S., Bryson, E. A., Cordelieres, F. P., Connors, N. C., Datta, S. R., Finkbeiner, S., Greenberg, M. E., and Saudou, F. (2002). The IGF-1/Akt pathway is neuroprotective in Huntington's disease and involves Huntingtin phosphorylation by Akt. *Dev Cell*, 2(6):831–837.

Jones, J. I. and Clemmons, D. R. (1995). Insulin-like growth factors and their binding proteins: biological actions. *Endocr Rev*, 16(1):3–34.

Kar, S., Poirier, J., Guevara, J., Dea, D., Hawkes, C., Robitaille, Y., and Quirion, R. (2006). Cellular distribution of insulin-like growth factor-II/mannose-6-phosphate receptor in normal human brain and its alteration in Alzheimer's disease pathology. *Neurobiol Aging*, 27(2):199–210.

Katsoyannis, P. G. (1967). Synthetic insulins. *Recent Prog Horm Res*, 23:505–563.

Khandwala, H. M., McCutcheon, I. E., Flyvbjerg, A., and Friend, K. E. (2000). The effects of insulin-like growth factors on tumorigenesis and neoplastic growth. *Endocr Rev*, 21(3):215–244.

Kiely, P. A., Sant, A., and O'Connor, R. (2002). RACK1 Is an Insulin-like Growth Factor 1 (IGF-1) Receptor-interacting Protein That Can Regulate IGF-1-mediated Akt Activation and Protection from Cell Death. *J Biol Chem*, 277(25):22581–22589.

Kiess, W., Yang, Y., Kessler, U., and Hoeflich, A. (1994). Insulin-like growth factor II (IGF-II) and the IGF-II/mannose-6-phosphate receptor: the myth continues. *Horm Res*, 41 Suppl 2:66–73.

Lie, Z., Zhang, W., and Sima, A. (2003). C-peptide enhances insulin-mediated cell growth and protection against high glucose-induced apoptosis in SH-SY5Y cells. *Diabetes Metab Res Rev*, 19(5):375–385.

Logan, A., Gonzalez, A. M., Hill, D. J., Berry, M., Gregson, N. A., and Baird, A. (1994). Coordinated pattern of expression and localization of insulin-like growth factor-II (IGF-II) and IGF-binding protein-2 in the adult rat brain. *Endocrinology*, 135(5):2255–2264.

Meinsma, D., Scheper, W., Holthuizen, P. E., Van den Brande, J. L., and Sussenbach, J. S. (1992). Site-specific cleavage of IGF-II mRNAs requires sequence elements from two distinct regions of the IGF-II gene. *Nucleic Acids Res*, 20(19):5003–5009.

Miyamoto, S., Yano, K., Sugimoto, S., Ishii, G., Hasebe, Takahiro Endoh, Y., Kodama, K., Goya, M., Chiba, T., and Ochiai, A. (2004). Matrix Metalloproteinase-7 Facilitates Insulin-Like Growth Factor Bioavailability through Its Proteinase Activity on Insulin-Like Growth Factor Binding Protein 3. *Cancer Res*, 64(2):665–671.

Nakae, J., Kido, Y., and Accili, D. (2001). Distinct and overlapping functions of insulin and IGF-I receptors. *Endocr Rev*, 22(6):818–835.

Near, S. L., Whalen, L. R., Miller, J. A., and Ishii, D. N. (1992). Insulin-like growth factor II stimulates motor nerve regeneration. *Proc Natl Acad Sci U S A*, 89(24):11716–11720.

Pedersen, M. V., Kohler, L. B., Ditlevsen, D. K., Li, S., Berezin, V., and Bock, E. (2004). Neuritogenic and survival-promoting effects of the P2 peptide derived from a homophilic binding site in the neural cell adhesion molecule. *J Neurosci Res*, 75(1):55–65.

Poduslo, J. F., Curran, G. L., Wengenack, T. M., Malester, B., and Duff, K. (2001). Permeability of proteins at the blood-brain barrier in the normal adult mouse and double transgenic mouse model of Alzheimer's disease. *Neurobiol Dis*, 8(4):555–567.

Pollak, M. N., Schernhammer, E. S., and Hankinson, S. E. (2004). Insulin-like growth factors and neoplasia. *Nat Rev Cancer*, 4(7):505–518.

Rinderknecht, E. and Humbel, R. E. (1978a). Primary structure of human insulin-like growth factor II. *FEBS Lett*, 89(2):283–286.

Rinderknecht, E. and Humbel, R. E. (1978b). The amino acid sequence of human insulin-like growth factor I and its structural homology with proinsulin. *J Biol Chem*, 253(8):2769–2776.

Ronn, L. C., Ralets, I., Hartz, B. P., Bech, M., Berezin, A., Berezin, V., Moller, A., and Bock, E. (2000). A simple procedure for quantification of neurite outgrowth based on stereological principles. *J Neurosci Methods*, 100(1-2):25–32.

Roth, B. V., Burgisser, D. M., Luthi, C., and Humbel, R. E. (1991). Mutants of human insulin-like growth factor II: expression and characterization of analogs with a substitution of TYR27 and/or a deletion of residues 62-67. *Biochem Biophys Res Commun*, 181(2):907–914.

Sakano, K., Enjoh, T., Numata, F., Fujiwara, H., Marumoto, Y., Higashihashi, N., Sato, Y., Perdue, J. F., and Fujita-Yamaguchi, Y. (1991). The design, expression, and characterization of human insulin-like growth factor II (IGF-II) mutants specific for either the IGF-II/cation-independent mannose 6-phosphate receptor or IGF-I receptor. *J Biol Chem*, 266(31):20626–20635.

Salmon, W. D. J. and Daughaday, W. H. (1957). A hormonally controlled serum factor which stimulates sulfate incorporation by cartilage in vitro. *J Lab Clin Med*, 49(6):825–836.

Schousboe, A., Frandsen, A., and Drejer, J. (1989). Evidence for evoked release of adenosine and glutamate from cultured cerebellar granule cells. *Neurochem Res*, 14(9):871–875.

Scott, C. D. and Firth, S. M. (2004). The role of the M6P/IGF-II receptor in cancer: tumor suppression or garbage disposal? *Horm Metab Res*, 36(5):261–271.

Shafqat, J., Melles, E., Sigmundsson, K., Johansson, B., Ekberg, K., Alvelius, G., Henriksson, M., Johansson, J., Wahren, J., and Jornvall, H. (2006). Proinsulin C-peptide elicits disaggregation of insulin resulting in enhanced physiological insulin effects. *Cell Mol Life Sci*, page Epub ahead of print.

Shaw, G., Morse, S., Ararat, M., and Graham, F. L. (2002). Preferential transformation of human neuronal cells by human adenoviruses and the origin of HEK 293 cells. *FASEB J*, 16(8):869–871.

Skene, J. H. (1989). Axonal growth-associated proteins. *Annu Rev Neurosci*, 12:127–156.

Steiner, D. F. (1969). Proinsulin and the biosynthesis of insulin. *N Engl J Med*, 280(20):1106–1113.

Steiner, D. F., Cunningham, D., Spigelman, L., and Aten, B. (1967). Insulin biosynthesis: evidence for a precursor. *Science*, 157(789):697–700.

Stewart, C. E. and Rotwein, P. (1996). Growth, differentiation, and survival: multiple physiological functions for insulin-like growth factors. *Physiol Rev*, 76(4):1005–1026.

Stockhorst, U., de Fries, D., Steingrueber, H.-J., and Scherbaum, V. A. (2004). Insulin and the CNS: effects on food intake, memory, and endocrine parameters and the role of intranasal insulin administration in humans. *Physiol Behav*, 83(1):47–54.

Trejo, J. L., Carro, E., Garcia-Galloway, E., and Torres-Aleman, I. (2004). Role of insulin-like growth factor I signaling in neurodegenerative diseases. *J Mol Med*, 82(3):156–162.

Valentinis, B. and Baserga, R. (2001). IGF-I receptor signalling in transformation and differentiation. *Mol Pathol*, 54(3):133–137.

van Buul-Offers, S. C., de Haan, K., Reijnen-Gresnigt, M. G., Meinsma, D., Jansen, M., Oei, S. L., Bonte, E. J., Sussenbach, J. S., and Van den Brande, J. L. (1995). Overexpression of human insulin-like growth factor-II in transgenic mice causes increased growth of the thymus. *J Endocrinol*, 144(3):491–502.

van Dam, P. S. and Aleman, A. (2004). Insulin-like growth factor-I, cognition and brain aging. *Eur J Pharmacol*, 490(1-3):87–95.

Vasilcanu, D., Weng, W.-H., Girnita, A., Lui, W.-O., Vasilcanu, R., Axelson, M., Larsson, O., Larsson, C., and Girnita, L. (2006). The insulin-like growth factor-1 receptor inhibitor PPP produces only very limited resistance in tumor cells exposed to long-term selection . *Oncogene*, 22(25):3186–3195.

Walenkamp, M. J. E., Karperien, M., Pereira, A. M., Hilhorst-Hofstee, Y., van Doorn, J., Chen, J. W., Mohan, S., Denley, A., Forbes, B., van Duyvenvoorde, H. A., van Thiel, S. W., Sluimers, C. A., Bax, J. J., de Laat, J. A. P. M., Breuning, M. B., Romijn, J. A., and Wit, J. M. (2005). Homozygous and heterozygous expression of a novel insulin-like growth factor-I mutation. *J Clin Endocrinol Metab*, 90(5):2855–2864.

Wilcox, G. (2005). Insulin and insulin resistance. *Clin Biochem Rev*, 26(2):19–39.

Woods, K. A., Camacho-Hubner, C., Barter, D., Clark, A. J., and Savage, M. O. (1997). Insulin-like growth factor I gene deletion causing intrauterine growth retardation and severe short stature. *Acta Paediatr Suppl*, 423:39–45. Case Reports.

Wozniak, M., Rydzewski, B., Baker, S. P., and Raizada, M. K. (1993). The cellular and physiological actions of insulin in the central nervous system. *Neurochem Int*, 22(1):1–10.

Ye, P., Li, L., Richards, R. G., DiAugustine, R. P., and D'Ercole, A. J. (2002). Myelination is altered in insulin-like growth factor-I null mutant mice. *J Neurosci*, 22(14):6041–6051.

Yin, Q. W., Johnson, J., Prevette, D., and Oppenheim, R. W. (1994). Cell death of spinal motoneurons in the chick embryo following deafferentation: rescue effects of tissue extracts, soluble proteins, and neurotrophic agents. *J Neurosci*, 14(12):7629–7640.

Zahn, H. (2000). My journey from wool research to insulin. *J Pept Sci*, 6(1):1–10. Biography.

Appendix A

Growth factors sensorgrams

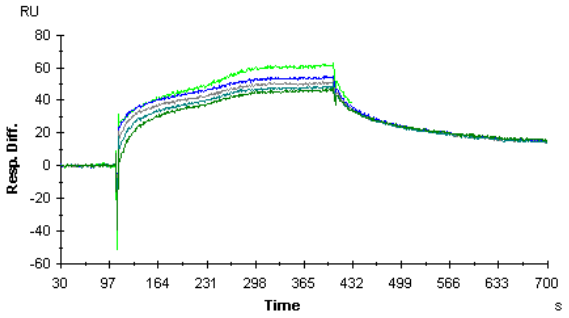

(a) IGF-IR

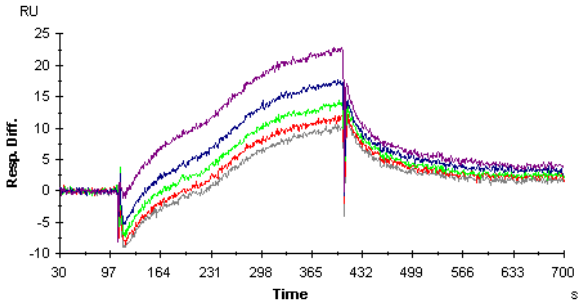

(b) IGF-IIR

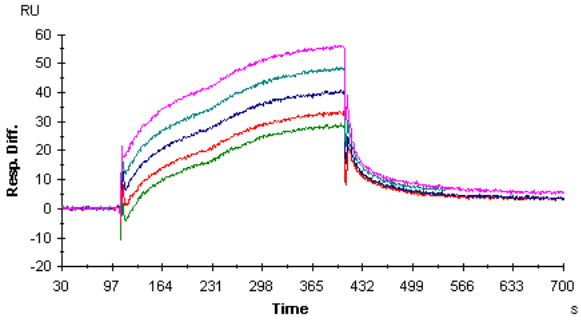

(c) IR

Figure A.1: IGF-I binding to the insulin/IGF receptors. IGF-IR, IGF-IIR and IR-A were immobilized on a sensor chip CM4 to a final density of 1200, 2000 and 1600 RU, respectively. The binding is expressed in resonance units and corresponds to the difference in binding to the flow cell with immobilized protein and the reference flow cell. Injections of 50, 100, 200, 400, 800 and 1600 μM IGF-I in HBS-EP buffer were made at flow rate 20 μl/min. The injection of 1600 μM IGF-I over the chip resulted in a poor sensorgram due to air bubbles in the buffer.

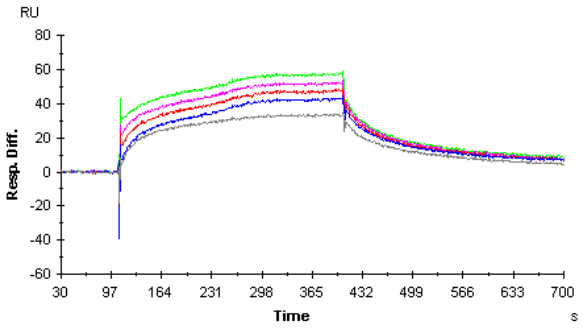

(a) IGF-IR

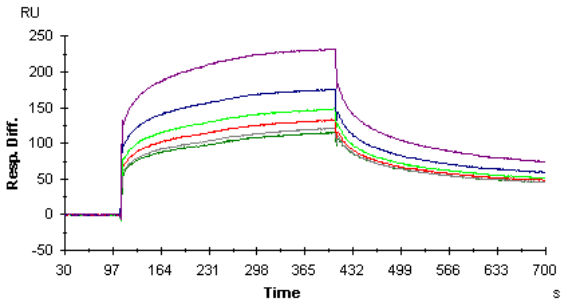

(b) IGF-IIR

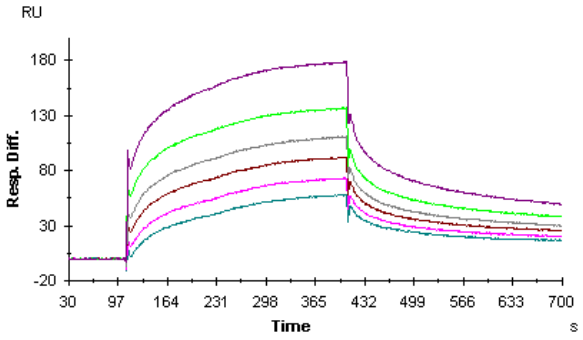

(c) IR

Figure A.2: IGF-II binding to the insulin/IGF receptors. IGF-IR, IGF-IIR and IR-A were immobilized on a sensor chip CM4 to a final density of 1200, 2000 and 1600 RU, respectively. The binding is expressed in resonance units and corresponds to the difference in binding to the flow cell with immobilized protein and the reference flow cell. Injections of 50, 100, 200, 400, 800 and 1600 μM IGF-I in HBS-EP buffer were made at flow rate 20 μl/min. The injection of 1600 μM IGF-II over the IGF-IR resulted in a poor sensorgram due to air bubbles in the buffer.

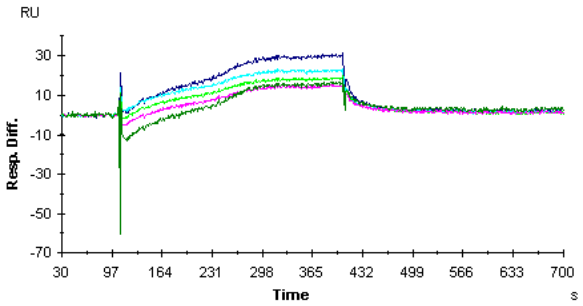

(a) IGF-IR

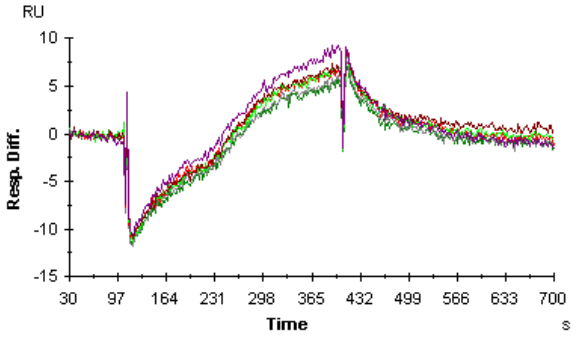

(b) IGF-IIR

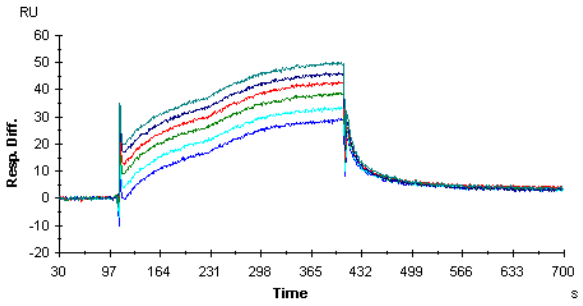

(c) IR

Figure A.3: Insulin binding to the insulin/IGF receptors. IGF-IR, IGF-IIR and IR-A were immobilized on a sensor chip CM4 to a final density of 1200, 2000 and 1600 RU, respectively. The binding is expressed in resonance units and corresponds to the difference in binding to the flow cell with immobilized protein and the reference flow cell. Injections of 50, 100, 200, 400, 800 and 1600 μM IGF-I in HBS-EP buffer were made at flow rate 20 μl/min. The injection of 1600 μM insulin over the IGF-IR resulted in a poor sensorgram due to air bubbles in the buffer.